Title: Proinsulin protects against age-related cognitive loss through anti-inflammatory convergent pathways.

Authors: Rubén Corpas[1]*, Alberto M. Hernández-Pinto[2]*, David Porquet[1], Catalina Hernández-Sánchez[2,3], Fatima Bosch[3,4], Arantxa Ortega-Aznar[5], Francesc Comellas[6], Enrique J. de la Rosa[2&], Coral Sanfeliu[1,7&]

Affiliations:
[1]Institut d'Investigacions Biomèdiques de Barcelona (IIBB), Consejo Superior de Investigaciones Científicas, 08036 Barcelona, Spain.
[2]3D Lab (Development, Differentiation and Degeneration), Department of Cellular and Molecular Medicine, Centro de Investigaciones Biológicas, Consejo Superior de Investigaciones Científicas, 28040 Madrid, Spain.
[3]Centro de Investigación Biomédica en Red de Diabetes y Enfermedades Metabólicas Asociadas (CIBERDEM), ISCIII, Madrid, Spain.
[4]Center of Animal Biotechnology and Gene Therapy and Department of Biochemistry and Molecular Biology, School of Veterinary Medicine, Universitat Autònoma de Barcelona, 08193 Bellaterra, Spain.
[5]Department of Pathology, Vall d'Hebron University Hospital, 08035 Barcelona, Spain.
[6]Department of Applied Mathematics IV, Universitat Politècnica de Catalunya, 08034 Barcelona, Spain.
[7]Institut d'Investigacions Biomèdiques August Pi i Sunyer (IDIBAPS), 08036 Barcelona, Spain.
[*, &] Equal first and senior contributors respectively

Corresponding authors:
Coral Sanfeliu
IIBB-CSIC, IDIBAPS
c/ Rosselló 161, 6th floor, 08036 Barcelona, Spain.
Phone: +34 933638338
Fax: +34 933638301
Email: coral.sanfeliu@iibb.csic.es

Enrique J. de la Rosa
CIB-CSIC
c/ Ramiro de Maeztu 9, 28040 Madrid, Spain.
Phone: +34 918373112
Fax: +34 915360432
Email: ejdelarosa@cib.csic.es

Abstract

Brain inflammaging is increasingly considered as contributing to age-related cognitive loss and neurodegeneration. Despite intensive research in multiple models, no clinically effective pharmacological treatment has been found yet. Here, in the mouse model of brain senescence SAMP8, we tested the effects of proinsulin, a promising neuroprotective agent that was previously proven to be effective in mouse models of retinal neurodegeneration. Proinsulin is the precursor of the hormone insulin but also upholds developmental physiological effects, particularly as a survival factor for neural cells. Adeno-associated viral vectors of serotype 1 bearing the human proinsulin gene were administered intramuscularly to obtain a sustained release of proinsulin into the blood stream, which was able to reach the target area of the hippocampus. SAMP8 mice and the control strain SAMR1 were treated at 1 month of age. At 6 months, behavioral testing exhibited cognitive loss in SAMP8 mice treated with the null vector. Remarkably, the cognitive performance achieved in spatial and recognition tasks by SAMP8 mice treated with proinsulin was similar to that of SAMR1 mice. In the hippocampus, proinsulin induced the activation of neuroprotective pathways and the downstream signaling cascade, leading to the decrease of neuroinflammatory markers. Furthermore, the decrease of astrocyte reactivity was a central effect, as demonstrated in the connectome network of changes induced by proinsulin. Therefore, the neuroprotective effects of human proinsulin unveil a new pharmacological potential therapy in the fight against cognitive loss in the elderly.

Title: Proinsulin protects against age-related cognitive loss through anti-inflammatory convergent pathways.

Authors: Rubén Corpas[1]*, Alberto M. Hernández-Pinto[2]*, David Porquet[1], Catalina Hernández-Sánchez[2,3], Fatima Bosch[3,4], Arantxa Ortega-Aznar[5], Francesc Comellas[6], Enrique J. de la Rosa[2&], Coral Sanfeliu[1,7&]

Affiliations:
[1]Institut d'Investigacions Biomèdiques de Barcelona (IIBB), Consejo Superior de Investigaciones Científicas, 08036 Barcelona, Spain.
[2]3D Lab (Development, Differentiation and Degeneration), Department of Cellular and Molecular Medicine, Centro de Investigaciones Biológicas, Consejo Superior de Investigaciones Científicas, 28040 Madrid, Spain.
[3]Centro de Investigación Biomédica en Red de Diabetes y Enfermedades Metabólicas Asociadas (CIBERDEM), ISCIII, Madrid, Spain.
[4]Center of Animal Biotechnology and Gene Therapy and Department of Biochemistry and Molecular Biology, School of Veterinary Medicine, Universitat Autònoma de Barcelona, 08193 Bellaterra, Spain.
[5]Department of Pathology, Vall d'Hebron University Hospital, 08035 Barcelona, Spain.
[6]Department of Applied Mathematics IV, Universitat Politècnica de Catalunya, 08034 Barcelona, Spain.
[7]Institut d'Investigacions Biomèdiques August Pi i Sunyer (IDIBAPS), 08036 Barcelona, Spain.

*, & Equal first and senior contributors respectively

Corresponding authors:
Coral Sanfeliu
IIBB-CSIC, IDIBAPS
c/ Rosselló 161, 6th floor, 08036 Barcelona, Spain.
Phone: +34 933638338
Fax: +34 933638301
Email: coral.sanfeliu@iibb.csic.es

Enrique J. de la Rosa
CIB-CSIC
c/ Ramiro de Maeztu 9, 28040 Madrid, Spain.
Phone: +34 918373112
Fax: +34 915360432
Email: ejdelarosa@cib.csic.es

Abstract

Brain inflammaging is increasingly considered as contributing to age-related cognitive loss and neurodegeneration. Despite intensive research in multiple models, no clinically effective pharmacological treatment has been found yet. Here, in the mouse model of brain senescence SAMP8, we tested the effects of proinsulin, a promising neuroprotective agent that was previously proven to be effective in mouse models of retinal neurodegeneration. Proinsulin is the precursor of the hormone insulin but also upholds developmental physiological effects, particularly as a survival factor for neural cells. Adeno-associated viral vectors of serotype 1 bearing the human proinsulin gene were administered intramuscularly to obtain a sustained release of proinsulin into the blood stream, which was able to reach the target area of the hippocampus. SAMP8 mice and the control strain SAMR1 were treated at 1 month of age. At 6 months, behavioral testing exhibited cognitive loss in SAMP8 mice treated with the null vector. Remarkably, the cognitive performance achieved in spatial and recognition tasks by SAMP8 mice treated with proinsulin was similar to that of SAMR1 mice. In the hippocampus, proinsulin induced the activation of neuroprotective pathways and the downstream signaling cascade, leading to the decrease of neuroinflammatory markers. Furthermore, the decrease of astrocyte reactivity was a central effect, as demonstrated in the connectome network of changes induced by proinsulin. Therefore, the neuroprotective effects of human proinsulin unveil a new pharmacological potential therapy in the fight against cognitive loss in the elderly.

Keywords: proinsulin; therapy; adeno-associated virus vector; cognitive loss; inflammaging

Abbreviations: A2M, α-2-macroglobulin; Aβ**,** amyloid β peptides; AβPP**,** amyloid β protein precursor; AAV, adeno-associated virus; AD, Alzheimer's disease; Akt, protein kinase B; ANOVA, analysis of variance; ATF1, activating transcription factor 1; BDNF**,** brain-derived neurotrophic factor; cDNA, complementary DNA; CRE, cAMP response element; CREB**,** cAMP response element-binding protein; ELISA, enzyme-linked immunosorbent assay; ERK, extracellular signal-regulated kinase; GAPDH, glyceraldehyde-3-phosphate dehydrogenase; GFAP, glial fibrillary acidic protein; GSK3-β; Glycogen synthase kinase 3 β; hPi, human proinsulin; Iba1, ionized calcium-binding adapter molecule 1; IGF, insulin-like

growth factors; IL-1β, interleukin 1 β; IL1R, interleukin 1 receptor type I; i.p., intraperitoneally; LTP, long-term potentiation; MWM, Morris water maze; NFκB, Nuclear factor κB p65 subunit; NORT, novel object recognition test; OLT, Novel object location test; p-, phosphorylated-; PI3K, phosphatidylinositol-3; qPCR, quantitative polymerase chain reaction; RIPA buffer, radioimmunoprecipitation assay buffer; SAMR1, senescence-accelerated mouse resistant 1; SAMP8, senescence-accelerated mouse-prone 8; s.c., subcutaneous; SEM, standard error of the mean; TNFα, Tumor necrosis factor α.

Introduction

Cognitive deficits associated with normal aging are exacerbated in the case of precocious aging or some neurodegenerative diseases (Deak et al., 2016). The prevalence of these conditions and the lack of clinically effective treatments drive the exploration of any available potential therapy. Proinsulin is a signaling protein with demonstrated neuroprotective properties beyond its nature as the precursor of the hormone insulin (de la Rosa and de Pablo, 2011; Steiner et al., 1967). A potential autocrine/paracrine effect of insulin/proinsulin in the brain has been suspected for some time, because moderate insulin/proinsulin levels were found in the brain independently of peripheral levels (Havrankova et al., 1978). At present, local production has been fully corroborated in brain tissue and cultured neurons (de Pablo and de la Rosa, 1995; Nemoto et al., 2014). Specific functions of insulin in brain include regulation of food intake, body weight, reproduction, and glycemic control in the hypothalamus, in addition to the promotion of learning and memory in the hippocampus (Ghasemi et al., 2013; Wada et al., 2005). Efficient insulin signaling is essential for healthy brain aging (Taguchi and White, 2008). The impairment of glucose metabolism and other insulin signaling pathways found in the Alzheimer's disease (AD) brain (Chami et al., 2016) has led to the study of insulin as a potential therapeutic agent against AD (Chen et al., 2016). Remarkably, its precursor, proinsulin, has gained recognition as a bioactive molecule beyond its role as a prohormone (Hernández-Sánchez et al., 2006). Early work demonstrated that the family of proinsulin, insulin, and insulin-like growth factors (IGF) modulates neuronal survival, proliferation, and differentiation during embryonic development (de Pablo and de la Rosa, 1995). Proinsulin may act in coordination with or independently of insulin and IGF to regulate specific pathways of embryonic neural cell death (Chavarría et al., 2007; Valenciano et al., 2006). Besides this developmental role, proinsulin exerts neuroprotective effects in animal models of the human disease retinitis pigmentosa, a retinal neurodegenerative condition causing vision loss (Corrochano et al., 2008; Fernández-Sánchez et al., 2012; Isiegas et al., 2016). Although the physiological relevance of proinsulin in adult mammals has not yet been elucidated, it appears as a promising neuroprotective agent meriting its being tested in diverse scenarios (de la Rosa and de Pablo, 2011). Specifically, proinsulin may have a potential pharmacological use under neural insulin-resistance conditions and in preventing abnormally increased neuronal cell death, as occurs in AD.

A widely used mouse model in the study of age-related neurodegeneration is the senescence-accelerated mouse-prone 8 (SAMP8). This mouse strain is a spontaneous model of senescence that demonstrates age-related brain pathologies and cognitive loss (Tomobe and Nomura, 2009). The defective learning and memory capacities of SAMP8 mice have been shown in different experimental tasks, including hippocampus-based spatial learning and memory and object recognition tasks (Dobarro et al., 2013; López-Ramos et al., 2012; Miyamoto et al., 1986; Wang et al., 2009; Yanai and Endo, 2016). Pathological changes are mainly present in the hippocampal area and include the following: (i) reduced synaptic plasticity with impaired long-term potentiation (LTP) (López-Ramos et al., 2012; Taniguchi et al., 2015) and lower activation of plasticity pathways (Li et al., 2009; Lin et al., 2014); (ii) increased levels of hyperphosphorylated tau (p-tau) with tau-related enzyme disorder (Álvarez-García et al., 2006; Canudas et al., 2005; Dobarro et al., 2013); (iii) higher accumulation of amyloid β peptides (Aβ) (Dobarro et al., 2013; Kumar et al., 2009; Zhang et al., 2011) which would be caused by an abnormally elevated synthesis of Aβ protein precursor (AβPP) (Griñán-Ferré et al., 2016; Morley et al., 2000) in addition to disturbances in the blood-brain barrier (Banks et al., 2011); (iv) oxidative stress (Álvarez-García et al., 2006; Butterfield et al., 1997; Morley et al., 2012); and (v) increased inflammation (Álvarez-López et al., 2014; Griñán-Ferré et al., 2016; Tha et al., 2000).

In this work, we assessed the therapeutic potential of proinsulin against cognitive loss and age-related neurodegeneration in the SAMP8 mouse model. To obtain a sustained chronic treatment, human proinsulin (hPi) was delivered into the blood stream through administration of recombinant adeno-associated viral (AAV) vectors of serotype 1 in the skeletal muscle. SAMP8 mice, as well as control senescence-accelerated mouse resistant 1 (SAMR1) mice, underwent muscle injection with AAV-hPi or control AAV-null vectors. For the experimental treatment, hPi, instead of mouse proinsulin, was chosen. This is an important requisite to obtain a proof of concept valid for human therapy. Nevertheless, the amino acid identity between human and the two mouse proinsulin proteins (there are two insulin genes in rodents) is high (~80%), allowing for the experimental use of hPi in mice (Supplementary Table 1). We have previously demonstrated that chronic production of hPi in skeletal muscle induced sustained levels of hPi and neuroprotective effects in a rat model of retinitis pigmentosa (Fernández-Sánchez et al., 2012). Our aim in this work was to extend the proof of concept of proinsulin as a neuroprotective agent to the complex scenario of age-related cognitive loss with a focus on hippocampal changes.

1. Materials and Methods

1.1. Animals and experimental design

Male mice of the strains SAMP8 and SAMR1 were used in the present study. Animal handling and experimental procedures were approved by the Ethics Committee for Animal Experimentation (CEEA) of the University of Barcelona (UB) [Ref: DAAM-6921, CEEA, UB, Barcelona, Spain], in accordance with Spanish legislation and the European Union (EU) Directive 2010/63/EU for animal experiments. Original breeding couples of SAMP8 and SAMR1 mice were obtained from the Council for SAM Research, Kyoto, Japan. Animal breeding, treatment, and behavioral studies were performed at UB animal house. Mice were maintained in Makrolon® cages under standard laboratory conditions of food and water ad libitum, 22 ± 2°C, and 12h:12h light-dark cycles.

Mice received a single intramuscular AAV-hPi or control (AAV-null) injection (see Section 1.2) at 1 month of age. Experimental groups were the following: SAMR1-null, N = 15; SAMR1-hPi, N = 20; SAMP8-null, N = 22; and SAMP8-hPi, N = 25. Animals were tested for behavioral and cognitive changes at 6 months of age. Peripheral blood and hippocampus brain tissues were obtained at termination.

An additional group of 3-month-old animals (SAMR1, N = 5; and SAMP8, N = 5) were utilized to check diffusion in the hippocampus and the possible metabolic effects of hPi after a subcutaneous (s.c.) bolus injection of 20 or 40 µg of hPi. Blood, hippocampus, and retina were obtained for analysis 2 h after injection.

1.2. Generation of adeno-associated viral vectors and mouse administration

Recombinant AAV serotype 1 viral (AAV1) vectors bearing the hPi complementary DNA (cDNA) under control of the cytomegalovirus promoter (AAV-hPi vector) or without hPi cDNA (AAV-null vector) were generated in the Center of Animal Biotechnology and Gene Therapy at the Universitat Autònoma de Barcelona. Vectors were produced by triple transfection of HEK293 cells with (i) a plasmid carrying the AAV *rep2* and *cap1* genes; (ii) a plasmid carrying the expression cassette flanked by the AAV2 viral Inverted Terminal Repeats (ITRs); and (iii) a plasmid carrying the adenovirus helper functions. AAV vectors were purified with an optimized method based on two consecutive cesium chloride gradients, dialyzed against PBS, filtered and stored at -80ºC until use (Ayuso et al., 2010). Titers of viral genomes were determined by quantitative polymerase chain reaction (qPCR) following

established protocols (Lock et al., 2010). AAV-hPi was injected intramuscularly at a dose of 0.72 x 10^9 vector genomes/g of body weight into SAMP8 and SAMR1 mice. Control animals received the same dose of AAV-null. Body weight was 23.07 ± 0.76 and 22.39 ± 0.57 g, for SAMR1 and SAMP8 mice, respectively; therefore they received an average of 16.6 x 10^9 and 16.1 x 10^9 vector genomes per mouse, respectively. The total dose of vectors was distributed between the gastrocnemius muscles of both hind limbs. AAV transduction of non-dividing cells, such as the skeletal muscle cells and liver cells, is predominantly non-integrative and supports long-term transgene expression, as demonstrated in studies with experimental animals (Arruda et al., 2010; Bernardes de Jesús et al., 2012; Binny et al., 2012; Callejas et al., 2013; Haurigot et al., 2010; Jaén et al., 2017; Nathwani et al., 2011) and in clinical studies (Buchlis et al., 2012; Nathwani et al., 2014).

1.3. Testing of cognitive and non-cognitive behavior

Cognitive changes were evaluated by three tests. (i) The *Novel object recognition test (NORT)* was employed to evaluate recognition memory based on the spontaneous tendency of rodents to spend more time exploring a novel than a familiar object. Animals were placed in the middle of a black maze with two arms angled at 90º (arms of 25 cm x 5 cm; 20-cm-high walls). After 2 previous days of a 10-min habituation in the empty maze, the animals were submitted to a 10-min acquisition trial in the presence of two identical novel objects (A1 + A2) placed at the end of each arm. A 10-min retention trial occurred 2 h later, replacing object A2 with object B. Another 10-min retention trial took place 24 h later, replacing object A1 with object C. Discrimination index was calculated as (tN–tF)/(tN+tF) where tN is time spent exploring the new object and tF is time spent exploring the familiar object (Bevins and Besheer, 2006; Vogel-Ciernia and Wood, 2014). The criterion used to score object exploration was that the mouse touched the object while looking at it or sniffed the object maintaining a distance of less than or equal to 2 cm between the nose and the object (Ennaceur and Delacour, 1988). (ii) The *Novel object location test (OLT)* was employed to evaluate spatial memory and discrimination. This test is based on the spontaneous tendency of rodents to spend more time exploring a novel than a familiar object, and also to recognize when an object has been relocated. The test is performed in a black open-field box (30 cm x 40 cm; 30-cm-high walls). Habituation to the apparatus has performed for 10 min on the day prior the acquisition trial. On that day, mice were allowed to explore, for 5 min, two identical objects (A1 + A2) that were placed in the corners of the experimental apparatus. Two h later, the test trial was conducted for 5 min with one of the objects (A2) moved to a different

location (A2'), while the other object (A1) remained in the same position. Discrimination index was calculated as (tD–tND)/(tD+tND) where tD is time spent exploring the displaced object (A2') and tND is time spent exploring the non-displaced object (A1) (Murai et al., 2007; Vogel-Ciernia and Wood, 2014). (iii) The *Morris water maze (MWM) test* was employed to evaluate spatial learning and memory. Briefly, animals were trained to locate a hidden platform 10 cm in diameter in a circular water tank (100 cm in diameter and 40-cm-high walls, with 25ºC opaque water, surrounded by black curtains) by relying on distinctive landmarks as visual cues. Acquisition consisted of 1 day of cue learning and 6 days of place learning, with 4 trials per day. The scape platform was made visible with a flag during the cue learning; this was a control condition to test that the animals had similar motor and visual capabilities (Vorhees and Williams, 2006). To notice that SAMP8 mice sensorimotor performance deteriorates with age at a higher pace than in SAMR1 mice (Markowska et al., 1998). However, the previous visual platform test might reduce the progression of the acquisition curve with the hidden platform. On day 7, after one place-learning trial, the platform was removed and the mice performed a 60-sec probe trial to test learning retention. A single learning trial was introduced to facilitate the memory response of animals whereas it did not change the response of impaired animals (Morris, 1984). A computerized tracking system (SMART; Panlab, Barcelona, Spain) allowed escape latency during the learning tasks to be measured, along with time spent in each pool quadrant after removal of the platform in the probe trial.

Non-cognitive behavior was tested to discard unwanted effects of the treatment. A *Battery of sensorimotor tests* permitted evaluating of reflexes (visual reflex and posterior limb-extension reflex), motor coordination and equilibrium (distance covered on a rod), and prehensility and muscle strength (distance and latency on falling from a metal wire). Motor activity, exploration, and emotionality were assessed by the analysis of patterns of horizontal and vertical activities in the *Open field test*. Neophobia for a new home cage was assessed by corner and rearing patterns in the *Corner test*. These non-cognitive tests were performed as previously described (García-Mesa et al., 2012); see complete description in Supplementary methods.

All behavioral testing was carried out during the first hours of the light period, from 09:00 h to 14:00 h local time.

At the completion of the behavioral testing, blood serum samples were obtained, animals were euthanized and the brain preserved for further analysis as described below.

1.4. Proinsulin and insulin levels, and glycaemia

The usage of hPi allows for unequivocally detection and distinction of the pharmacologically tested molecule from the endogenously produced. Circulating and tissue human proinsulin and insulin protein levels were determined with commercial Enzyme-linked immunosorbent assay (ELISA) kits, i.e., Human Total Proinsulin and Human Insulin (EZHI-15K and EZHI-14K, respectively, both from Merck, Millipore, Darmstadt, Germany), following the manufacturer's instructions. The kits are highly selective for the respective molecules. Serum and tissue preparation for ELISA was performed as previously described (Isiegas et al., 2016). Glycaemia was directly measured in a blood sample with the Glucocart™ Gmeter kit (A. Menarini Diagnostics, Ltd., Berkshire, UK).

1.5. Immunoblotting analysis

Levels of selected signaling proteins that may be related with proinsulin action were analyzed in the hippocampus, as the main target area for novel pro-cognitive therapy in SAMP8. Hippocampus tissue was homogenized in ice-cold Radioimmunoprecipitation assay (RIPA) buffer supplemented with protease and phosphatase inhibitors and analyzed for Western blot analysis by standard procedures (Revilla et al., 2014). Thirty micrograms of protein extract were employed to test the levels of the following proteins: phospho-Protein kinase B Ser473 (p-Akt), p-Akt Thr308, Akt, p-Extracellular signal-regulated kinase Thr202/Tyr204 (p-ERK), p-cAMP response element-binding protein Ser133 (p-CREB)/p-Activating transcription factor 1 Ser63 (p-ATF1), CREB and p-Nuclear factor κB p65 subunit Ser276 (p-NFκB) (antibody dilution 1:1,000, purchased from Cell Signaling, Danvers, MA, USA); pan-ERK (1:1,000; BD Biosciences, San Jose, CA, USA); Brain-derived neurotrophic factor (BDNF) and Glycogen synthase kinase 3 β Ser9 (p-GSK3-β) (1:1,000, Santa Cruz, Dallas, TX, USA); Synaptophysin (1:10,000; Dako, Glostrup, Denmark); Glial fibrillary acidic protein (GFAP), pan-Actin 20–33 and β-Tubulin (1:1,000, 1:10,000 and 1:10,000, respectively, Sigma-Aldrich, St Louis, MI, USA); Ionized calcium-binding adapter molecule 1 (Iba1) (1:2,000, Wako, Richmond, VA, USA); p-Tau Ser396 (1:500; Invitrogen, Thermo Fisher Scientific, Waltham, MA, USA); AβPP C-terminal fragment (1:1,000; Covance, Princeton, NJ, USA); and Glyceraldehyde-3-phosphate dehydrogenase (GAPDH) (1:2,000; Assay Designs, Ann Arbor, MI, USA). Secondary antibodies were horseradish peroxidase-conjugated (1:2,000; Amersham, Arlington Heights, IL, USA). The immunoreactive bands were detected by a chemiluminiscence method and digitized. Densitometric results were normalized to pan-Actin, β-Tubulin or GAPDH.

1.6. Histology and immunostaining

The brains of three mice per experimental group were histologically processed to confirm the presence of reactive astrocytes and/or microglia in the hippocampus. Mice were perfused with 4% paraformaldehyde in phosphate buffer under anesthesia of 10 mg/kg xylazine (Rompun 2%, Bayer, Leverkusen, Germany) intraperitoneally (i.p.) and 80 mg/kg ketamine (Ketolar 50 mg/mL, Pfizer, Alcobendas, Madrid, Spain) i.p. Brains were postfixed for 24 h, cryopreserved in 30% sucrose solution, and frozen on dry ice. Twenty-µm slices were double-stained with primary antibodies against GFAP (1:1000; Dako, Glostrup, Denmark) and Iba1 (1:500; Wako, Richmond, VA, USA). The secondary antibodies utilized included Alexa Fluor 488 and Alexa Fluor 546 (1:1,000; Molecular Probes, Thermo Fisher Scientific). Tissue sections were mounted on Mowiol® (Calbiochem, San Diego, CA, USA).

1.7. Real-time quantitative PCR

Total RNA was isolated from mouse hippocampus using the mirVana™ RNA Isolation Kit (Applied Biosystems, Carlsbad, CA, USA) following the manufacturer's instructions. RNA yield, purity and quality were determined employing a NanoDrop™ ND1000 spectrophotometer (Thermo Fisher Scientific). RNA with a 260/280 ratio of >1.9 was selected. Random-primed cDNA synthesis was performed using the Superscript III Kit and random primers (Thermo Fisher Scientific).

Gene expression was measured with the ABI Prism 7900HT Sequence Detection System using TaqMan FAM-labeled specific probes (Thermo Fisher Scientific). Genes and their corresponding TaqMan probes were the following: *A2m*, Mm00558642_m1; *Tnfα*, Mm00443260_g1; *Il1b*, Mm00434228_m1; *Il1r1*, Mm00434237_m1; and *Tbp*, Mm00446971_m1. Data were normalized to the expression of the TATA-binding protein gene (*Tbp*).

1.8. Statistics

Results were expressed as mean ± standard error of the mean (SEM). Data normality was tested by means of the Shapiro–Wilks test. Data were analyzed by two-way analysis of variance (ANOVA); factors were mouse strain and proinsulin treatment. Interaction and factor effects were analyzed for significance. Significant interaction was followed by simple main effect analysis. Association between pairs of variables was evaluated by Pearson correlation test; the weight of eventual spurious correlations was minimized through the

subsequent network analysis (see Section 1.9). *P*-values <0.05 were considered significant. Statistical analyses were performed using IBM SPSS Statistics ver. 22.0 software (IBM Corporation, Armonk, NY USA) and GraphPad Prism ver. 6.0 (GraphPad Software, Inc., CA USA).

1.9. Network analysis

Graph theory tools were used to jointly analyze the results of the main variables measured in the study, specifically those corresponding to cognition, plasticity, neuroprotection, inflammation, and pathology. Data of the additional mice utilized to test proinsulin delivery and the treatment effects on the peripheral metabolism of glucose were not included in the network analysis. Pairs of variables showing statistically significant correlations (*P*-values < 0.05) were selected to build a network, as described elsewhere (García-Mesa et al., 2016). Briefly, the correlation network was analyzed with the PageRank centrality algorithm (Page et al., 1999) using Mathematica ver. 9 software (Wolfram Research, Champaign, IL USA). This algorithm assigns a weight to each network node. Node weight is the PageRank of the node and ranks its importance within the set of nodes. A node (variable) that has links (correlations between pairs of variables), either directly or through other nodes, to many nodes that have a high PageRank value receives a high PageRank itself and it is said to be more central in the network.

2. **Results**

2.1. Serum and hippocampus proinsulin levels

A single administration of AAV-hPi into skeletal muscle induced the sustained production of hPi and its delivery into the blood circulation. Peripheral-blood serum hPi levels at the end of the five-month study were 24.32 ± 8.26 pM and 13.06 ± 2.97 pM, for SAMR1-hPi and SAMP8-hPi, respectively. No hPi was detected in the serum of mice injected with the control vector, AAV-null. hPi concentration in the hippocampus of AAV-hPi-treated mice was found under the detection threshold of the assay. However, hPi levels were readily detectable in the hippocampus after a single *in-vivo* administration of a s.c. bolus of 20 or 40 μg hPi in both SAMP8 and SAMR1 mice (Fig. 1A). Levels in the retina were used for comparison (Fig. 1A), because we have previously demonstrated that hPi produced in mouse skeletal muscle exerts a neuroprotective role on the retinal tissue (Corrochano et al., 2008). Furthermore, there was a positive correlation between hPi concentration in hippocampus and serum upon

the bolus administration (Fig. 1B) [r = 0.79, N = 10, P = 0.006]. There also was a positive correlation between hPi levels in hippocampus and retina (Fig. 1C) [r = 0.80, N = 10, P = 0.009]. Incidentally, the serum levels found in the SAMP8 mice were always lower, independently of the treatment method. We may speculate that senescence alterations reported in SAMP8 kidney and liver may influence hPi metabolism (Baltanás et al., 2013; Bayram et al., 2013). However, this aspect is out of the scope of this work.

The glycaemia of the AAV-hPi treated mice, exhibiting levels of hPi in the picomolar range, was not altered in comparison to untreated animals, as previously reported (Corrochano et al., 2008; Fernández-Sánchez et al., 2012). Accordingly, no differences in animal weight were observed in the AAV-hPi treated mice respect to the AAV-null treated ones after five months. The body weight for the different experimental groups at termination was as follows: 37.09 ± 1.53 and 39.81 ± 1.02 g, for SAMR1-null and SAMR1-hPi mice, respectively; and 32.25 ± 0.66 and 33.43 ± 1.50 g, for SAMP8-null and SAMP8-hPi mice, respectively. Only when the mice were subjected to a very high doses (20 or 40-µg bolus) of hPi, which resulted in levels of hPi in the nanomolar range, they presented a modest decrease in glycaemia that, however, remained above critical hypoglycemia values (data not shown). This could be partially due to that human insulin was found in serum at concentrations of 4.7% (1-14%) of those of hPi. Remarkably, we have never been able to detect human insulin in the serum or the tissues of AAV-hPi -treated mice.

2.2. Proinsulin induced the Akt pathway in SAMP8 hippocampus

We assayed, by immunoblotting, the activation of any pathway characteristic of proinsulin signaling (Malaguarnera et al., 2012). Skeletal muscle expression of hPi induced a significant increase of the levels of Akt phosphorylated at Ser^{473} in the hippocampus of both the SAMP8 and SAMR1 mouse strains (Fig. 2A). Our long-term, sustained, *in vivo* treatment displayed a well-established sign of activation of the phosphatidylinositol-3 kinase (PI3K)/Akt pathway (Kumar et al., 2007). Two-way ANOVA demonstrated an effect of the factor treatment for Akt^{Ser473} levels [F(1,22) = 12.2, P = 0.002]. Next, we tested the levels of the downstream transcription factors of the CREB/ATF family, which is involved in plasticity signaling. CREB and ATF1 are highly related at the functional and structural levels, and their phosphorylated forms were recognized by the same antibody (Fig. 2B). Proinsulin did not induce a recovery of the p-CREB levels found decreased in SAMP8 mice [factor strain, F(1, 22) = 11.1, P = 0.003]. However, proinsulin induced a general increase in p-ATF1 [factor

treatment, F(1, 23) = 4.5, *P* = 0.045]. These results support that hPi reaches the target tissue and activates the Akt signaling pathway.

Immunoblotting analysis of other key molecules involved in trophic factor signaling (synaptophysin, pro-BDNF, BDNF, p-ERK, ERK, p-GSK3β and p-NFκB) and in SAMP8 pathology (AβPP and p-tau) did not show statistically significant changes induced by proinsulin (Supplementary Fig. 1). However, the expression levels of these proteins exhibited significant correlations with other variables in the statistical study (Supplementary Table 2); therefore, they were included in the network analysis.

2.3. Proinsulin protected against inflammaging in SAMP8 hippocampus

Next, we analyzed the gene-expression of inflammatory markers and the effects of proinsulin on these. The hippocampus of SAMP8-null mice demonstrated more prominent signs of neuroinflammation than that of SAMR1-null mice, as expected. The expression of the pro-inflammatory cytokines Tumor necrosis factor α (TNFα) and Interleukin 1 β (IL-1β), and the cytokine transporter α-2-Macroglobulin (A2M) were found increased by 85%, 50% and 50% respectively in the hippocampus of SAMP8-null when compared with SAMR1 mice, whereas Interleukin 1 receptor type I (IL1R) did not change. Skeletal muscle administration of AAV-hPi in SAMP8 mice induced a decrease of TNFα, IL-1β and A2M expression to SAMR1 levels as well as a 22% decrease of IL1R expression (Fig. 3A). The analysis of the expression pattern of inflammatory genes showed an effect of interaction between the mouse strain and the gene treatment [two-way repeated measures ANOVA, strain x treatment interaction F(1,23) = 6.4, *P* = 0.019]. Subsequent analysis showed a simple main effect of strain factor in the AAV-null mice (*P* = 0.007) and of treatment factor in the SAMP8 mice (*P* = 0.010). Therefore, proinsulin decreased neuroinflammation in the hippocampus of SAMP8 mice.

The analysis of the glial cells, astrocytes and microglia, that are involved in the neuroinflammatory processes demonstrated a significant astrocyte activation in SAMP8. The GFAP level determined by immunoblotting was higher in SAMP8 than SAMR1 hippocampus (Fig. 3B). Remarkably, proinsulin treatment decreased GFAP levels in both SAMP8 and SAMR1 strains, driving astrocytes of SAMP8-hPi mice to normal reactivity levels. ANOVA indicated an effect of strain [F(1,33) = 10.00, *P* = 0.0033] and treatment [F(1,33) = 8.6, *P* = 0.006]. Immunostaining with GFAP antibody showed a lower presence of reactive astrocytes in the hippocampus of SAMP8-hPi mice than SAMP8-null ones by visual inspection of the microscope slides (Fig. 3C), thus reinforcing the Western blot results. In the case of microglia, no differences were detected by Iba1 immunoblotting (Fig. 3 D) or

immunostaining (Fig. 3E), but a non-significant trend to increase this reactive marker by AAV-hPi treatment.

2.4. Proinsulin protected against cognitive deficits in SAMP8 mice

Therapy with AAV-hPi induced important neuroprotective effects that counteracted SAMP8 deficits in learning and memory. Five months after treatment application, cognitive testing in three different paradigms involving hippocampus-based behavior, with NORT (Clark et al., 2000; Broadbent et al., 2010), OLT (Assini et al., 2009; Barker and Warburton, 2015) and MWM test (Laeremans et al., 2015; Riedel et al., 1999) was performed. Six-month-old SAMP8-null mice showed cognitive loss, whilst SAMP8-hPi mice showed cognitive capacities at the level of SAMR1 mice. No effects were induced in SAMR1 mice.

In the NORT (Fig. 4A), all mice demonstrated no preference in exploration of identical objects during task acquisition. SAMP8-null mice, those injected with control AAV-null, exhibited a deficit of recognition memory in the NORT, while SAMP8-hPi mice showed capacity of discriminating novel-type from familiar objects at 2 h and at 24 h, as did SAMR1 mouse groups. ANOVA indicated effect of strain [$F(1,76) = 5.3$, $P = 0.024$] and treatment [$F(1,76) = 9.7$, $P = 0.002$] at 2 h time and effect of strain [$F(1,76) = 8.4$, $P = 0.005$] at 24 h. Therefore, AAV-hPi treatment generally improved cognitive performance in both mouse strains at the 2 h time recall of recognition memory. However, the cognitive improvement trend clearly shown by SAMP8-hPi mice at 24 h did not reach statistical significance.

In the OLT (Fig. 4B), the mice demonstrated similar exploration of the objects at both locations during task acquisition. After 2 h, SAMP8-null mice exhibited impaired ability to discriminate the displaced object, while SAMP8-hPi and both groups of SAMR1 mice showed the capacity to recall the initial position of the object. ANOVA indicated an effect of strain [$F(1,38) = 5.3$, $P = 0.026$] and treatment [$F(1,38) = 8.6$, $P = 0.006$]. Therefore, AAV-hPi therapy increased the cognitive ability in the OLT paradigm of both mouse strains. Remarkably, SAMR1-hPi OLT average index duplicated that of SAMR1-null group.

In the MWM test (Fig. 4C), the learning acquisition curve of SAMP8-hPi showed a trend to improvement by proinsulin as compared with SAMP8-null. Two-way repeated-measures ANOVA revealed an effect of strain [$F(1,78) = 11.7$, $P = 0.001$], whereas the interaction of strain x treatment factors reached borderline significance [$F(1,78) = 3.7$, $P = 0.057$]. In the memory retrieval, SAMP8-hPi demonstrated total recovery of cognitive capacity as compared with the low performance of SAMP8-null. ANOVA showed strain and treatment effects and interaction between both factors [$F(1,67) = 6.0$, $P = 0.017$, $F(1,67) = 6.5$, $P =$

0.013 and F(1,67) = 4.4, P = 0.040, respectively]. No effect of mouse strain or treatment factors was found in the analysis of the swimming speed throughout the acquisition days or during the 60-sec probe trial.

Motor activity and ambulation was tested in both mouse strains to discard any local effect of the vector injection. Furthermore, SAMP8 mice are reported to display non-cognitive alterations, such as sensorimotor impairment, hyperactivity, and reduced anxiety-like behavior compared with SAMR1 (Markowska et al., 1998; Miyamoto et al., 1992; Sawano et al., 2013). These non-cognitive behaviors were also tested for proinsulin-induced changes. We found that transduction of gastrocnemius muscle cells with AAV-hPi did not impaired the sensorimotor responses of the mice, nor induced substantial effects on exploratory and emotionality-based behaviors in SAMP8 or SAMR1 mice (Supplementary Fig. 2). Non-cognitive behavior was not included in the graph theory study.

2.5. Astrocyte reactivity emerged as a central node of inflammaging

Correlation analysis including all mice of the four experimental groups showed a total of 59 significant correlations (links) between 28 variables (nodes) of the study (Supplementary Table 2A), which were utilized to build a network (Fig. 5). The PageRank algorithm allowed ordering the variables according to their centrality in the network. GFAP (PageRank #1) was the variable most highly connected with many other important nodes. The following variables were the removal test in the MWM (PageRank #2), p-CREB/CREB hippocampus level (PageRank #3), NORT at 2 h (PageRank #4), pro-BDNF hippocampus level (PageRank #5) and serum levels of hPi (PageRank #6) (See figure legend for the full PageRank list). GFAP correlated negatively with some learning and memory variables, neuroplasticity markers, and neuroprotective signaling pathways, and correlated positively with neuroinflammatory markers and amyloid and tau pathology. These and other connections in the network demonstrated that improvement of cognition is generally linked with proinsulin treatment, with decreased astrocyte reactivity and inflammation markers, and with increased neuroplasticity markers. The markers of the neuroprotective signaling pathways analyzed showed robust connectivity among themselves and with neuroplasticity and serum levels of hPi. Correlation analysis performed separately for SAMR1 mice (Supplementary Table 2B) lacked most correlations of learning and memory parameters because of the absence of cognitive deficiencies, but generally maintained those between parameters of neuroplasticity markers and neurotrophic signaling. The corresponding network analysis (Supplementary Fig. 3A) showed high weight of the nodes of hippocampal protein levels: p-CREB (Page

Rank #1), p-NFκB (Page Rank #2), p-ATF1 (Page Rank #3), p-CREB/CREB (Page Rank #4), p-GSK3β (Page Rank #5) and synaptophysin (PageRank #6) (See figure legend for the full PageRank list).

Correlation analysis performed separately for SAMP8 mice (Supplementary Table 2C) showed an increased number of correlations between the pathological traits of the mice, including cognition parameters, hippocampal protein markers and neuroinflammatory markers. The subsequent network analysis (Supplementary Fig. 3B) maintained GFAP as the variable with highest centrality (Page Rank #1), followed by the removal test in the MWM (PageRank #2), NORT at 2 h (PageRank #3), synaptophysin hippocampus level (PageRank #4), expression hippocampus levels of IL-1β (Page Rank #5) and p-Akt-Thr308 hippocampus levels (Page Rank #6) (See figure legend for the full PageRank list).

3. **Discussion**

Pharmacological levels of circulating hPi, obtained through intramuscular administration of AAV-hPi vectors in the SAMP8 murine model of precocious aging and cognitive loss, demonstrated the potential of this signaling molecule of the insulin family for the treatment of age-related cognitive pathologies. Six-month old SAMP8 mice, sustainably exposed to proinsulin, exhibited preserved spatial memory and recognition memory, two paradigms that require a fully functional hippocampus. The use of AAV vectors is emerging as a promising approach for neurological disorders (for review, see: Choundhurt et al., 2016). Here we assayed a further advantageous approach with the transduction of an accessible peripheral tissue.

Hippocampus is an essential brain structure in memory formation and in maintaining memories throughout the lifetime (Bataglia et al., 2011). Damage within this region of the central nervous system and its neuronal networks, including connections to directly related cortical areas, is a common feature in neurodegeneration and AD (Moodley and Chan, 2014). Moreover, subtle dysfunctions in the hippocampus are thought to cause age-related memory impairment across species (Leal and Yassa, 2015). Our model system, the SAMP8 mouse, presents early deficits in hippocampal plasticity and functionality that are considered the major cause of their cognitive loss (Taniguchi et al., 2015; Bayod et al., 2015; Tomobe et al., 2007; Lopez-Ramos et al., 2012). Preservation of learning and memory abilities after proinsulin therapy may indicate functional improvement of hippocampus circuitry and also beneficial effects in related cortical brain areas. Cortical areas functionally connected with

the hippocampus that are relevant for the recognition memory analyzed here, in addition to spatial memory, are the perirhinal and the medial prefrontal cortices (Barker and Warburton, 2011, 2015). Therefore, proinsulin generally reduced brain senescence pathology in these mice.

Insulin receptors are distributed in discrete areas of the brain, being the hippocampus one of the regions with highest levels (Doré et al., 1997; Marks et al., 1990). Insulin receptor signaling plays a central role in several critical Central Nervous System functions including energy homeostasis, food intake and cognition. Activation of hippocampal insulin receptors has been associated to enhancement of learning and memory functions (reviewed by Biessels and Reagan, 2015). The receptors mediating proinsulin action are not fully characterized. However, it has been reported that proinsulin preferentially exerts its biological effects through binding to insulin receptor isoform A (IR-A) while displaying low affinity for the more metabolic insulin receptor isoform B (Malaguarnera et al., 2012). IR-A is predominantly expressed during prenatal life, whereas in adult tissues, it is especially expressed in neural tissue (Hernández-Sánchez et al., 2008), including hippocampus (Belfiore et al., 2009). Consequently, proinsulin and insulin activate similar neuroprotective pathways in the brain, including the PI3K/Akt route (van der Heide et al., 2006), with negligible impact of proinsulin on glucose homeostasis. Our observations agree with the expected proinsulin mode of action. Analysis of signaling pathways that may underlie proinsulin neuroprotection revealed the involvement of Akt pathway in the hippocampus, as demonstrated by the increase in Akt phosphorylation in both SAMR1-hPi and SAMP8-hPi. Similarly, proinsulin stimulates the Akt pathway and preserves neuronal cells in a neurodegenerative model of retinitis pigmentosa (Isiegas et al., 2016). Supporting activation of the Akt pathway by proinsulin in hippocampus, we found activation of downstream transcription factor ATF1. The members of the CREB/ATF family include CREB, cAMP response element modulator (CREM) and ATF1. These are activated, directly or indirectly, by Akt. Then, they bind to CRE in the promoter regions of specific genes and activate their transcription in response to external stimuli. These transcription factors induce neuronal gene expression in the process of information processing and memory consolidation (Lonze and Ginty, 2002; Pittenger et al., 2002). Here we found activation of ATF1, but no significant changes in CREB. Noticeably, ATF1 function has been shown to compensate for CREB deficiency in mouse brain (Hummler et al., 1994). Therefore, here, proinsulin increased hippocampus plasticity mainly through ATF1. Furthermore, ATF1 is implicated in the regulation of many genes in addition to cAMP-inducible genes (Hai et al., 1989). Proinsulin activated downstream Akt pathway in

both strains SAMR1 and SAMP8. Furthermore, control SAMP8 mice did not show a down regulation of this pathway. Taking into account that some degree of memory improvement was also detected in proinsulin-treated SAMR1 mice, we can suggest that proinsulin induced a general pro-cognitive effect. This cognitive enhancement might be at least partially independent of the presence of previous cognitive pathologies.

SAMP8 mice undergo a moderate level of systemic and brain inflammation as an element of their precocious senescence (Álvarez-López et al., 2014; Griñán-Ferré et al., 2016; Tha et al., 2000; Wang et al., 2015). Proinsulin protected against signs of neuroinflammation in the SAMP8 hippocampus, both decreasing generation of pro-inflammatory cytokines and reducing astrocyte reactivity. Proinsulin-induced cognitive improvement in SAMP8 mice may be at least partially mediated by decreasing IL-1β and TNFα expression to normal levels. IL-1β impairs synaptic plasticity by blocking LTP. The underlying mechanisms suggested here comprise an increase of reactive oxygen species followed by activation of the stress-activated protein kinases (Vereker et al., 2000) and inhibition of calcium currents (Cunningham et al., 1996). The significance of IL-1β in hippocampus neural plasticity is supported by the high concentration of its receptor IL1R in hippocampal neurons (Ban et al., 1991). The other main cytokine tested, TNFα, similarly impairs LTP (Cunningham et al., 1996). Furthermore, TNFα may potentiate excitotoxicity through inhibition of glutamate uptake (Zhou et al., 2005). IL-1β and TNFα are synthesized by reactive glial cells, both microglia and astrocytes; their expression and that of their receptors are high, especially in hippocampus among the brain areas (Hopkins et al., 1995). A2M has not been, to our knowledge, previously determined in SAMP8. Glycoprotein A2M is a proteinase inhibitor and a specific carrier of cytokines, including TNFα and IL-1β. A2M can inhibit the proteolytic degradation of pro-inflammatory cytokines leading to sustained inflammatory processes (Gourine et al., 2002). A2M is synthesized in the brain primarily by astrocytes, and its receptor is expressed in neurons and astrocytes (Moestrup et al., 1992). A2M is increased in the AD brain, where it can be neurotoxic to neurons (Kovacs, 2000). The significant contribution of neuroinflammatory processes to age-related cognitive impairment was further corroborated by the discovery of several polymorphisms in pro-inflammatory genes, including the genes of TNFα, IL-1β and A2M, which increase the risk of AD (McGeer and McGeer, 2001). The observed anti-inflammatory effects of proinsulin in the hippocampus are in agreement with that of insulin in peripheral tissues in which insulin seems to modulate vascular permeability and cytokine production by an uncharacterized mechanism (Kothari et al., 2016).

SAMP8 mice showed reactive astrocytes in the hippocampus. Previous authors have demonstrated that the number of astrocytic cell bodies remained constant with age in the SAMP8 hippocampus despite increased GFAP immunoreactivity, thus indicating a change in hypertrophic reactivity (Sawano et al., 2013). SAMP8 reactive astrocytes appear to play a significant role in exaggerated and long-lasting brain inflammatory responses against stress factors and subsequent impairment of memory in SAMP8. In addition, SAMP8 astrocytes expressed degenerative markers (Díez-Vives et al., 2009) and dysfunctions leading to a reduction of vital support to neurons *in vitro* (García-Matas et al., 2008). Astrocyte reactivity involves morphological, transcriptional and functional changes (Ben Haim et al., 2016). Interaction among the pathways triggering astrocyte reactivity and neuroprotective pathways activated by proinsulin such as PI3K/Akt would return astrocytes to their physiologically normal state. It is noteworthy that these were responsive to the lowering of their reactivity by proinsulin, as measured by the decrease in GFAP expression. Microglia, another player in neuroinflammation did not show significant changes in activation after proinsulin treatment or in baseline conditions in SAMP8.

In conclusion, the pharmacological circulating levels of hPi obtained through intramuscular AAV-hPi administration allowed for a sustained, systemic, low level of proinsulin able to reach the mouse brain. Proinsulin treatment led to significant protection, lasting several months, against cognitive impairment in the SAMP8 mouse model of senescence and decreased the signs of brain inflammaging. Inhibition of astrocyte reactivity comprised a central event in the connectivity network built with the data of the study. The successful outcome of proinsulin therapy in SAMP8 mice opens new pharmacological avenues in the treatment of inflammaging and age-related neurodegeneration.

Disclosure statement

The authors have no actual or potential conflicts of interest.

Funding resources

This work was supported by grants: CSD2010-00045 to CS and EJdlR, from the Spanish Ministerio de Economía y Competitividad (MINECO), SAF2016-77703-C2-2-R to CS from MINECO and European Regional Development Fund (ERDF), and TRACE (PET08-0282) to

FB and EJdlR, from the Spanish Ministerio de Ciencia e Innovación (MICINN). FB is a recipient of an ICREA Academia award, Generalitat de Catalunya, Spain.

Acknowledgements

We thank Prof. Flora de Pablo for critical reading of the manuscript, and Cayetana Murillo and José Luís Martínez for technical assistance. We also wish to thank Dr Emili Corbella for his help with the statistical analyses and Dr Virginia Haurigot for helpful discussion.

Supplementary material

Supplementary Methods. Non-cognitive tests.

Supplementary Table 1. Proinsulin sequence shows high homology between human and mouse forms.

Supplementary Table 2. Pearson correlation results of variables of the study.

Supplementary Figure 1. Hippocampus levels of selected proteins involved in neurotrophic signaling and SAMP8 pathology that were not modified by proinsulin.

Supplementary Figure 2. Non-cognitive behavior was barely modified by proinsulin.

Supplementary Figure 3. Network analysis performed separately with SAMR1 and SAMP8 mice.

References

Álvarez-García, O., Vega-Naredo. I., Sierra. V., Caballero. B., Tomás-Zapico. C., Camins. A., García. J.J., Pallàs, M., Coto-Montes. A., 2006. Elevated oxidative stress in the brain of senescence-accelerated mice at 5 months of age. Biogerontology 7, 43-52.

Alvarez-López, M.J., Molina-Martínez, P., Castro-Freire, M., Cosín-Tomás, M., Cristòfol, R., Párrizas, M., Escorihuela, R.M., Pallàs, M., Sanfeliu, C., Kaliman, P., 2014. Rcor2 underexpression in senescent mice: a target for inflammaging? J. Neuroinflammation 11, 126.

Arruda, V.R., Stedman, H.H., Haurigot, V., Buchlis, G., Baila, S., Favaro, P., Chen, Y., Franck, H.G., Zhou, S., Wright, J.F., Couto, L.B., Jiang, H., Pierce, G.F., Bellinger, D.A., Mingozzi, F., Nichols, T.C., High, K.A., 2010. Peripheral transvenular delivery of adeno-associated viral vectors to skeletal muscle as a novel therapy for hemophilia B. Blood 115, 4678-4688.

Assini, F.L., Duzzioni, M., Takahashi, R.N., 2009. Object location memory in mice: pharmacological validation and further evidence of hippocampal CA1 participation. Behav. Brain. Res. 204, 206-211.

Ayuso, E., Mingozzi, F., Montane, J., Leon, X., Anguela, X.M., Haurigot, V., Edmonson, S.A., Africa, L., Zhou, S., High, K.A., Bosch, F., Wright, J.F., 2010. High AAV vector purity results in serotype- and tissue-independent enhancement of transduction efficiency. Gene Ther. 17, 503-510.

Baltanás, A., Solesio, M.E., Zalba, G., Galindo, M.F., Fortuño, A., Jordán, J., 2013. The senescence-accelerated mouse prone-8 (SAM-P8) oxidative stress is associated with upregulation of renal NADPH oxidase system. J. Physiol. Biochem. 69, 927-935.

Ban, E., Milon, G., Prudhomme, N., Fillion, G., Haour, F., 1991. Receptors for interleukin1 (α and β) in mouse brain: Mapping and neuronal localization in hippocampus. Neuroscience 43, 2130.

Banks, W.A., Kumar, V.B., Farr, S.A., Nakaoke, R., Robinson, S.M., Morley, J.E., 2011. Impairments in brain-to-blood transport of amyloid-β and reabsorption of cerebrospinal fluid in an animal model of Alzheimer's disease are reversed by antisense directed against amyloid-β protein precursor. J. Alzheimers Dis. 23, 599-605.

Barker, G.R., Warburton, E.C., 2011. When is the hippocampus involved in recognition memory? J Neurosci. 31, 10721-10731.

Barker, G.R., Warburton, E.C., 2015. Object-in-place associative recognition memory depends on glutamate receptor neurotransmission within two defined hippocampal-cortical circuits: a critical role for AMPA and NMDA receptors in the hippocampus, perirhinal, and prefrontal cortices. Cereb. Cortex 25, 472-481.

Battaglia, F.P., Benchenane, K., Sirota, A., Pennartz, C.M., Wiener, S.I., 2011. The hippocampus: hub of brain network communication for memory. Trends Cogn. Sci. 15, 310-318.

Bayod, S., Felice, P., Andrés, P., Rosa, P., Camins, A., Pallàs, M., Canudas, A.M., 2015. Downregulation of canonical Wnt signaling in hippocampus of SAMP8 mice. Neurobiol. Aging 36, 720-729.

Bayram, B., Nikolai, S., Huebbe, P., Ozcelik, B., Grimm, S., Grune, T., Frank, J., Rimbach, G., 2013. Biomarkers of oxidative stress, antioxidant defence and inflammation are altered in the senescence-accelerated mouse prone 8. Age (Dordr). 35, 1205-1217.

Bernardes de Jesus, B., Vera, E., Schneeberger, K., Tejera, A.M., Ayuso, E., Bosch, F., Blasco, M.A., 2012. Telomerase gene therapy in adult and old mice delays aging and increases longevity without increasing cancer. EMBO Mol. Med. 4, 691-704

Bevins, R.A., Besheer, J., 2006. Object recognition in rats and mice: a one-trial non-matching-to-sample learning task to study 'recognition memory'. Nat. Protoc. 1, 1306-1311.

Ben Haim, L., Carrillo-de Sauvage, M.A., Ceyzériat, K., Escartin, C., 2015. Elusive roles for reactive astrocytes in neurodegenerative diseases. Front. Cell Neurosci. 9, 278.

Belfiore, A., Frasca, F., Pandini, G., Sciacca, L., Vigneri, R., 2009. Insulin receptor isoforms and insulin receptor/insulin-like growth factor receptor hybrids in physiology and disease. Endocr. Rev. 30, 586-623.

Biessels, G.J., Reagan, L.P., 2015. Hippocampal insulin resistance and cognitive dysfunction. Nat. Rev. Neurosci. 16, 660-671.

Binny, C., McIntosh, J., Della Peruta, M., Kymalainen, H., Tuddenham, E.G., Buckley, S.M., Waddington, S.N., McVey, J.H., Spence, Y., Morton, C.L., Thrasher, A.J., Gray, J.T., Castellino, F.J., Tarantal, A.F., Davidoff, A.M., Nathwani, A.C., 2012. AAV-mediated gene transfer in the perinatal period results in expression of FVII at levels that protect against fatal spontaneous hemorrhage. Blood 119, 957-966.

Broadbent, N.J., Gaskin, S., Squire, L.R., Clark, R.E., 2010. Object recognition memory and the rodent hippocampus. Learn. Mem. 17, 5-11.

Buchlis, G., Podsakoff, G.M., Radu, A., Hawk, S.M., Flake, A.W., Mingozzi, F., High, K.A., 2012. Factor IX expression in skeletal muscle of a severe hemophilia B patient 10 years after AAV-mediated gene transfer. Blood 119, 3038-3041.

Butterfield, D.A., Howard, B.J., Yatin, S., Allen, K.L., Carney, J.M., 1997. Free radical oxidation of brain proteins in accelerated senescence and its modulation by N-tert-butyl-alpha-phenylnitrone. Proc. Natl. Acad. Sci. USA 94, 674-678.

Callejas, D., Mann, C.J., Ayuso, E., Lage, R., Grifoll, I., Roca, C., Andaluz, A., Ruiz-de Gopegui, R., Montané, J., Muñoz, S., Ferre, T., Haurigot, V., Zhou, S., Ruberte, J., Mingozzi, F., High, K.A., Garcia, F., Bosch, F., 2013. Treatment of diabetes and long-term survival after insulin and glucokinase gene therapy. Diabetes 62, 1718-1729.

Canudas, A.M., Gutierrez-Cuesta, J., Rodríguez, M.I., Acuña-Castroviejo, D., Sureda, F.X., Camins, A., Pallàs, M., 2005. Hyperphosphorylation of microtubule-associated protein tau in senescence-accelerated mouse (SAM). Mech. Ageing Dev. 126, 1300-1304.

Chami, B., Steel, A.J., De La Monte, S.M., Sutherland, G.T., 2016. The rise and fall of insulin signaling in Alzheimer's disease. Metab. Brain Dis. 31, 497-515.

Chavarría, T., Valenciano, A.I., Mayordomo, R., Egea, J., Comella, J.X., Hallböök, F., de Pablo, F., de la Rosa, E.J., 2007. Differential, age-dependent MEK-ERK and PI3K-Akt activation by insulin acting as a survival factor during embryonic retinal development. Dev. Neurobiol. 67, 1777-1788.

Chen, Y., Zhang, J., Zhang, B., Gong, C.X., 2016. Targeting Insulin Signaling for the Treatment of Alzheimer's Disease. Curr. Top. Med. Chem. 16, 485-492.

Clark, R.E., Zola, S.M., Squire, L.R., 2000. Impaired recognition memory in rats after damage to the hippocampus. J. Neurosci. 20, 8853-8860.

Choudhury, S.R., Hudry, E., Maguire, C.A., Sena-Esteves, M., Breakefield, X.O., Grandi, P., 2016. Viral vectors for therapy of neurologic diseases. Neuropharmacology in press, doi: 10.1016/j.neuropharm.2016.02.013.

Corrochano, S., Barhoum, R., Boya, P., Arroba, A.I., Rodríguez-Muela, N., Gómez-Vicente, V., Bosch, F., de Pablo, F., de la Villa, P., de la Rosa, E.J., 2008. Attenuation of vision loss and delay in apoptosis of photoreceptors induced by proinsulin in a mouse model of retinitis pigmentosa. Invest. Ophthalmol. Vis. Sci. 49, 4188-4194.

Cunningham, A.J., Murray, C.A., O'Neill, L.A., Lynch, M.A., O'Connor, J.J., 1996. Interleukin-1β (IL-1β) and tumour necrosis factor (TNF) inhibit long-term potentiation in the rat dentate gyrus in vitro. Neurosci. Lett. 203, 17-20.

de la Rosa, E.J., de Pablo, F., 2011. Proinsulin: from hormonal precursor to neuroprotective factor. Front. Mol. Neurosci. 4, 20.

de Pablo, F., de la Rosa, E.J., 1995. The developing CNS: a scenario for the action of proinsulin, insulin and insulin-like growth factors. Trends Neurosci. 18, 143-150.

Deak, F., Freeman, W.M., Ungvari, Z., Csiszar, A., Sonntag, W.E., 2016. Recent developments in understanding brain aging: Implications for Alzheimer's disease and vascular cognitive impairment. J. Gerontol. A Biol. Sci. Med. Sci. 71, 13-20.

Díez-Vives, C., Gay, M., García-Matas, S., Comellas, F., Carrascal, M., Abian, J., Ortega-Aznar, A., Cristòfol, R., Sanfeliu, C., 2009. Proteomic study of neuron and astrocyte cultures from senescence-accelerated mouse SAMP8 reveals degenerative changes. J. Neurochem. 111, 945-955.

Dobarro, M., Orejana, L., Aguirre, N. Ramírez, M.J., 2013. Propranolol restores cognitive deficits and improves amyloid and Tau pathologies in a senescence-accelerated mouse model. Neuropharmacology 64, 137-144.

Doré, S., Kar, S., Rowe, W., Quirion, R., 1997. Distribution and levels of [^{125}I]IGF-I, [^{125}I]IGF-II and [^{125}I]insulin receptor binding sites in the hippocampus of aged memory-unimpaired and -impaired rats. Neuroscience 80, 1033-1340.

Ennaceur, A., Delacour, J., 1988. A new one-trial test for neurobiological studies of memory in rats. I: behavioral data. Behav. Brain Res 31, 47–59.

Fernández-Sánchez, L., Lax, P., Isiegas, C., Ayuso, E., Ruiz, J.M., de la Villa, P., Bosch, F., de la Rosa, E.J., Cuenca, N., 2012. Proinsulin slows retinal degeneration and vision loss in the P23H rat model of retinitis pigmentosa. Hum. Gene Ther. 23, 1290-1300.

García-Matas, S., Gutierrez-Cuesta, J., Coto-Montes, A., Rubio-Acero, R., Díez-Vives, C., Camins, A., Pallàs, M., Sanfeliu, C., Cristòfol, R., 2008. Dysfunction of astrocytes in senescence-accelerated mice SAMP8 reduces their neuroprotective capacity. Aging Cell 7, 630-640.

García-Mesa, Y., Colie, S., Corpas, R., Cristòfol, R., Comellas, F., Nebreda, A.R., Giménez-Llort, L., Sanfeliu, C., 2016. Oxidative Stress Is a Central Target for Physical Exercise Neuroprotection Against Pathological Brain Aging. J. Gerontol. A Biol. Sci. Med. Sci. 71, 40-49.

García-Mesa, Y., Giménez-Llort, L., López, L.C., Venegas, C., Cristòfol, R., Escames, G., Acuña-Castroviejo, D., Sanfeliu, C., 2012. Melatonin plus physical exercise are highly neuroprotective in the 3xTg-AD mouse. Neurobiol. Aging 33, 1124.e13-29.

Ghasemi, R., Haeri, A., Dargahi L., Mohamed, Z., Ahmadiani, A., 2013. Insulin in the brain: sources, localization and functions. Mol. Neurobiol. 47, 145-171.

Gourine, A.V., Gourine, V.N., Tesfaigzi, Y., Caluwaerts, N., Van Leuven, F., Kluger, M.J., 2002. Role of α2-macroglobulin in fever and cytokine responses induced by lipopolysaccharide in mice. Am. J. Physiol. Regul. Integr. Comp. Physiol. 83, R218-226.

Griñán-Ferré, C., Palomera-Ávalos, V., Puigoriol-Illamola, D., Camins, A., Porquet, D., Plá, V., Aguado, F., Pallàs, M., 2016. Behaviour and cognitive changes correlated with hippocampal neuroinflammaging and neuronal markers in female SAMP8, a model of accelerated senescence. Exp. Gerontol. 80, 57-69.

Havrankova, J., Schmechel, D., Roth, J., Brownstein, M., 1978. Identification of insulin in rat brain. Proc. Natl. Acad. Sci. U S A. 75, 5737-5741.

Hai, T.W., Liu, F., Coukos, W.J., Green, M.R., 1989. Transcription factor ATF cDNA clones: an extensive family of leucine zipper proteins able to selectively form DNA-binding heterodimers. Genes Dev. 3, 2083-2090.

Haurigot, V., Mingozzi, F., Buchlis, G., Hui, D.J., Chen, Y., Basner-Tschakarjan, E., Arruda, V.R., Radu, A., Franck, H.G., Wright, J.F., Zhou, S., Stedman, H.H., Bellinger, D.A., Nichols, T.C., High, K.A., 2010. Safety of AAV factor IX peripheral transvenular gene delivery to muscle in hemophilia B dogs. Mol Ther. 18, 1318-1329.

Hernández-Sánchez, C., Mansilla, A., de la Rosa, E.J., de Pablo, F., 2006. Proinsulin in development: New roles for an ancient prohormone. Diabetologia 49, 1142-1150.

Hernández-Sánchez, C., Mansilla, A., de Pablo, F., Zardoya, R., 2008. Evolution of the insulin receptor family and of receptor isoform expression in vertebrates. Mol. Biol. Evol. 25, 1043-1053.

Hopkins, S.J., Rothwell, N.J., 1995. Cytokines and the nervous system. I: Expression and recognition. Trends Neurosci. 18, 83-88.

Hummler, E., Cole, T.J., Blendy, J.A., Ganss, R., Aguzzi, A., Schmid, W., Beermann, F., Schütz, G., 1994. Targeted mutation of the CREB gene: compensation within the CREB/ATF family of transcription factors. Proc. Natl. Acad. Sci. USA 91, 5647-5651.

Isiegas, C., Marinich-Madzarevich, J.A., Marchena, M., Ruiz, J.M., Cano, M.J., de la Villa, P., Hernández-Sánchez, C., de la Rosa, E.J., de Pablo, F., 2016. Intravitreal injection of Proinsulin-loaded microspheres delays photoreceptor cell death and vision loss in the rd10 mouse model of Retinitis Pigmentosa. Invest. Ophthalmol. Vis. Sci. 57, 3610-3618.

Jaén, M.A., Vilà, L., Elias, I., Jimenez, V., Rodó, J., Maggioni,L., Ruiz-de Gopegui, R., Garcia, M., Muñoz, S., Callejas, D., Ayuso, E., Ferré, T., Grifoll, I., Andaluz, A.,

Ruberte, J., Haurigot, V., Bosch, F., 2017. Long-term efficacy and safety of insulin and glucokinase gene therapy for diabetes: Eight-year follow-up in dogs. Mol. Ther. Methods Clin. Dev. 6, 1-7.

Kothari, V., Galdo, J.A., Mathews, S.T., 2016. Hypoglycemic agents and potential anti-inflammatory activity. J. Inflamm. Res. 9:27-38.

Kovacs, D.M., 2000. α2-Macroglobulin in late-onset Alzheimer's disease. Exp. Gerontol. 35, 473-479.

Kumar, N., Afeyan, R., Sheppard, S., Harms, B., Lauffenburger, D.A., 2007. Quantitative analysis of Akt phosphorylation and activity in response to EGF and insulin treatment. Biochem. Biophys. Res. Commun. 354, 14-20.

Kumar, V.B., Franko, M., Banks, W.A., Kasinadhuni, P., Farr, S.A., Vyas, K., Choudhuri, V., Morley, J.E., 2009. Increase in presenilin 1 (PS1) levels in senescence-accelerated mice (SAMP8) may indirectly impair memory by affecting amyloid precursor protein (APP) processing. J. Exp. Biol. 212, 494-498.

Laeremans, A., Sabanov, V., Ahmed, T., Nys, J., Van de Plas, B., Vinken, K., Woolley, D.G., Gantois, I., D'Hooge, R., Arckens, L., Balschun, D., 2015. Distinct and simultaneously active plasticity mechanisms in mouse hippocampus during different phases of Morris water maze training. Brain Struct. Funct. 220, 1273-1290.

Leal, S.L., Yassa, M.A., 2015. Neurocognitive aging and the hippocampus across species. Trends Neurosci. 38, 800-812.

Li, Q., Zhao, H.F., Zhang, Z.F., Liu, Z.G., Pei, X.R., Wang, J.B., Li, Y., 2009. Long-term green tea catechin administration prevents spatial learning and memory impairment in senescence-accelerated mouse prone-8 mice by decreasing Aβ1-42 oligomers and upregulating synaptic plasticity-related proteins in the hippocampus. Neuroscience 163, 741-749.

Lin, N., Pan, X.D., Chen, A.Q., Zhu, Y.G., Wu, M., Zhang, J., Chen, X.C., 2014. Tripchlorolide improves age-associated cognitive deficits by reversing hippocampal synaptic plasticity impairment and NMDA receptor dysfunction in SAMP8 mice. Behav. Brain Res. 258, 8-18.

Lock, M., McGorray, S., Auricchio, A., Ayuso, E., Beecham, E.J., Blouin-Tavel, V., Bosch, F., Bose, M., Byrne, B.J., Caton, T., Chiorini, J.A., Chtarto, A., Clark, K.R., Conlon, T., Darmon, C., Doria, M., Douar, A., Flotte, T.R., Francis, J.D., Francois, A., Giacca, M., Korn, M.T., Korytov, I., Leon, X., Leuchs, B., Lux, G., Melas, C., Mizukami, H., Moullier, P., Müller, M., Ozawa, K., Philipsberg, T., Poulard, K., Raupp, C., Rivière, C.,

Roosendaal, S.D., Samulski, R.J., Soltys, S.M., Surosky, R., Tenenbaum, L., Thomas, D.L., van Montfort, B., Veres, G., Wright, J.F., Xu, Y., Zelenaia, O., Zentilin, L., Snyder, R.O., 2010. Characterization of a recombinant adeno-associated virus type 2 Reference Standard Material. Hum. Gene Ther. 21, 1273-1285.

Lonze, B.E., Ginty, D.D., 2002. Function and regulation of CREB family transcription factors in the nervous system. Neuron 35, 605-623.

López-Ramos, J.C., Jurado-Parras, M.T., Sanfeliu, C., Acuña-Castroviejo, D., Delgado-García, J.M., 2012. Learning capabilities and CA1-prefrontal synaptic plasticity in a mice model of accelerated senescence. Neurobiol Aging 33, 627.e13-26.

Malaguarnera, R., Sacco, A., Voci, C., Pandini, G., Vigneri, R., Belfiore, A., 2012. Proinsulin binds with high affinity the insulin receptor isoform A and predominantly activates the mitogenic pathway. Endocrinology. 153, 2152-2163.

Markowska, A.L., Spangler, E.L., Ingram, D.K., 1998. Behavioral assessment of the senescence-accelerated mouse (SAM P8 and R1). Physiol. Behav. 64, 15-26.

Marks, J.L., Porte, D. Jr., Stahl, W.L., Baskin D.G., 1990. Localization of insulin receptor mRNA in rat brain by in situ hybridization. Endocrinology 127, 3234-3236.

McGeer, P.L., McGeer, E.G., 2001. Polymorphisms in inflammatory genes and the risk of Alzheimer disease. Arch. Neurol. 58, 1790-1792.

Miyamoto, M., Kiyota, Y., Nishiyama, M., Nagaoka, A., 1992. Senescence-accelerated mouse (SAM): age-related reduced anxiety-like behavior in the SAM-P/8 strain. Physiol. Behav. 51, 979-985.

Miyamoto, M., Kiyota, Y., Yamazaki, N., Nagaoka, A., Matsuo, T., Nagawa, Y., Takeda, T., 1986. Age-related changes in learning and memory in the senescence-accelerated mouse (SAM). Physiol. Behav. 38, 399-406.

Moestrup, S.K., Gliemann, J., Pallesen, G., 1992. Distribution of the α2-macroglobulin receptor/low density lipoprotein receptor-related protein in human tissues. Cell Tissue Res. 269, 375-382.

Moodley, K.K., Chan, D., 2014. The hippocampus in neurodegenerative disease. Front. Neurol. Neurosci. 34, 95-108.

Morley, J.E., Armbrecht, H.J., Farr, S.A., Kumar, V.B., 2012. The senescence accelerated mouse (SAMP8) as a model for oxidative stress and Alzheimer's disease. Biochim. Biophys. Acta 1822, 650-656.

Morley, J.E., Kumar, V.B., Bernardo, A.E., Farr, S.A., Uezu, K., Tumosa, N., Flood, J.F., 2000. β-Amyloid precursor polypeptide in SAMP8 mice affects learning and memory. Peptides 21, 1761-1767.

Morris, R., 1984. Developments of a water-maze procedure for studying spatial learning in the rat. J. Neurosci. Methods 11, 47-60.

Murai, T., Okuda, S., Tanaka, T., Ohta, H., 2007. Characteristics of object location memory in mice: Behavioral and pharmacological studies. Physiol. Behav. 90, 116-124.

Nathwani, A.C., Rosales, C., McIntosh, J., Rastegarlari, G., Nathwani, D., Raj, D., Nawathe, S., Waddington, S.N., Bronson, R., Jackson, S., Donahue, R.E., High, K.A., Mingozzi, F,, Ng, C.Y., Zhou, J., Spence, Y., McCarville, M.B., Valentine, M., Allay, J., Coleman, J., Sleep, S., Gray, J.T., Nienhuis, A.W., Davidoff, A.M., 2011. Long-term safety and efficacy following systemic administration of a self-complementary AAV vector encoding human FIX pseudotyped with serotype 5 and 8 capsid proteins. Mol. Ther. 19, 876-885.

Nathwani, A.C., Reiss, U.M., Tuddenham, E.G., Rosales, C., Chowdary, P., McIntosh, J., Della Peruta, M., Lheriteau, E., Patel, N., Raj, D., Riddell, A., Pie, J., Rangarajan, S., Bevan, D., Recht, M., Shen, Y.M., Halka, K.G., Basner-Tschakarjan, E., Mingozzi, F., High, K.A., Allay, J., Kay, M.A., Ng, C.Y., Zhou, J., Cancio, M., Morton, C.L., Gray, J.T., Srivastava, D., Nienhuis, A.W., Davidoff, A.M., 2014. Long-term safety and efficacy of factor IX gene therapy in hemophilia B. N Engl J Med. 371, 1994-2004.

Nemoto, T., Toyoshima-Aoyama, F., Yanagita, T., Maruta, T., Fujita, H., Koshida, T., Yonaha, T., Wada, A., Sawaguchi, A., Murakami, M., 2014. New insights concerning insulin synthesis and its secretion in rat hippocampus and cerebral cortex: Amyloid-β_{1-42}-induced reduction of proinsulin level via glycogen synthase kinase-3β. Cell Signal. 26, 253-259.

Page, L., Brin, S., Motwani, R., Winograd, T., 1999. The PageRank Citation Ranking: Bringing Order to the Web. Technical Report. Stanford InfoLab. http://ilpubs.stanford.edu:8090/422/.

Pittenger, C., Huang, Y.Y., Paletzki, R.F., Bourtchouladze, R., Scanlin, H., Vronskaya, S., Kandel, E.R., 2002. Reversible inhibition of CREB/ATF transcription factors in region CA1 of the dorsal hippocampus disrupts hippocampus-dependent spatial memory. Neuron 34, 447-462.

Revilla, S., Suñol, C., García-Mesa, Y., Giménez-Llort, L., Sanfeliu, C., Cristòfol, R., 2014. Physical exercise improves synaptic dysfunction and recovers the loss of survival factors in 3xTg-AD mouse brain. Neuropharmacology 81, 55-63.

Riedel, G., Micheau, J., Lam, A.G., Roloff, E.L., Martin, S.J., Bridge, H., de Hoz, L., Poeschel, B., McCulloch, J., Morris, R.G., 1999. Reversible neural inactivation reveals hippocampal participation in several memory processes. Nat. Neurosci. 2, 898-905.

Sawano, E., Negishi, T., Aoki, T., Murakami, M., Tashiro, T., 2013. Alterations in local thyroid hormone signaling in the hippocampus of the SAMP8 mouse at younger ages: association with delayed myelination and behavioral abnormalities. J. Neurosci. Res. 91, 382-392.

Steiner, D.F., Cunningham, D., Spigelman, L., Aten, B., 1967. Insulin biosynthesis: evidence for a precursor. Science 157, 697-700.

Taguchi, A., White, M.F., 2008. Insulin-like signaling, nutrient homeostasis, and life span. Annu. Rev. Physiol. 70, 191-212.

Taniguchi, S., Mizuno, H., Kuwahara, M., Ito, K., 2015. Early attenuation of long-term potentiation in senescence-accelerated mouse prone 8. Exp. Brain Res. 233, 3145-3152.

Tha, K.K., Okuma, Y., Miyazaki, H., Murayama, T., Uehara, T., Hatakeyama, R., Hayashi, Y., Nomura, Y., 2000. Changes in expressions of proinflammatory cytokines IL-1β, TNF-α and IL-6 in the brain of senescence accelerated mouse (SAM) P8. Brain Res. 885, 25-31.

Tomobe, K., Nomura, Y., 2009. Neurochemistry, neuropathology, and heredity in SAMP8: a mouse model of senescence. Neurochem. Res. 34, 660-669.

Tomobe, K., Okuma, Y., Nomura, Y., 2007. Impairment of CREB phosphorylation in the hippocampal CA1 region of the senescence-accelerated mouse (SAM) P8. Brain Res. 1141, 214-217.

van der Heide, L.P., Ramakers, G.M., Smidt, M.P., 2006. Insulin signaling in the central nervous system: learning to survive. Prog. Neurobiol. 79, 205-221.

Valenciano, A.I., Corrochano, S., de Pablo, F., de la Villa, P., de la Rosa, E.J., 2006. Proinsulin/insulin is synthesized locally and prevents caspase- and cathepsin-mediated cell death in the embryonic mouse retina. J. Neurochem. 99, 524-536.

Vereker, E., O'Donnell, E., Lynch, M.A., 2000. The inhibitory effect of interleukin-1β on long-term potentiation is coupled with increased activity of stress-activated protein kinases. J. Neurosci. 20, 6811-6819.

Vogel-Ciernia, A., Wood, M.A., 2014. Examining object location and object recognition memory in mice. Curr. Protoc. Neurosci. 2014, 69:8.31.1-17.

Vorhees, C.V., Williams, M.T., 2006. Morris water maze: procedures for assessing spatial and related forms of learning and memory. Nat. Protoc. 1, 848-858.

Wada, A., Yokoo, H., Yanagita, T., Kobayashi, H., 2005. New twist on neuronal insulin receptor signaling in health, disease, and therapeutics. J. Pharmacol. Sci. 99, 128-143.

Wang, F., Chen, H., Sun, X., 2009. Age-related spatial cognitive impairment is correlated with a decrease in ChAT in the cerebral cortex, hippocampus and forebrain of SAMP8 mice. Neurosci. Lett. 454, 212-217.

Wang, X., Puerta, E., Cedazo-Minguez, A., Hjorth, E., Schultzberg, M., 2015. Insufficient resolution response in the hippocampus of a senescence-accelerated mouse model - SAMP8. J. Mol. Neurosci. 55, 396-405.

Yanai, S., Endo, S., 2016. Early onset of behavioral alterations in senescence-accelerated mouse prone 8 (SAMP8). Behav. Brain Res. 308, 187-195.

Zhang, Y., He, J.S., Wang, X., Wang, J., Bao, F.X., Pang, S.Y., Yin, F., Hu, H.G., Peng, X.L., Sun, W.M., Zheng, Y.P., Hou, L.L., Hong, T., 2011. Administration of amyloid-β42 oligomer-specific monoclonal antibody improved memory performance in SAMP8 mice. J. Alzheimers Dis. 23, 551-561.

Zou, J.Y., Crews, F.T., 2005. TNFα potentiates glutamate neurotoxicity by inhibiting glutamate uptake in organotypic brain slice cultures: neuroprotection by NFκB inhibition. Brain Res. 1034, 11-24.

Figure legends

Figure 1. Human proinsulin levels after a subcutaneous bolus injection in SAMP8 and SAMR1 mice (A) Human proinsulin (hPi) injected subcutaneously at the indicated doses in SAMR1 and SAMP8 mice was detected by ELISA in blood serum, as well as in tissue extracts from hippocampus and retina. Values represent the mean ± SEM, $N = 3$. (B) Levels in the hippocampus correlated with those in blood serum. Individual mouse values are shown, $N = 10$. (C) Levels of hPi in the hippocampus correlated with those in the retina. Individual mouse values are shown, $N = 10$; see text for correlation values.

Figure 2. Proinsulin administered through an AAV vector in the skeletal muscle induced the Akt pathway and activated the plasticity transduction factor ATF1 in the hippocampus. (A) Increased ratio of p-Akt/Akt was found in the hippocampus of both 6-month-old SAMR1 and SAMP8 mice treated with AAV-hPi at 1 month of age. (B) AAV-hPi induced an increase in the ratio p-ATF1/CREB, although the increase in p-CREB/CREB ratio was not significant. In all cases, values represent the mean ± SEM. Statistics: two-way ANOVA; $^{\$}P < 0.05$, $^{\$\$}P < 0.01$ effect of factor treatment, $^{\&\&}P < 0.01$ effect of factor strain.

Figure 3. Proinsulin reduced astrocyte reactivity and neuroinflammation in the hippocampus of SAMP8 mice. (A) The genes *A2m, Tnfα, Il1β* and *Il1r1*, codifying for α-2-Macroglobulin (A2M), Tumor necrosis factor α (TNFα), Interleukin 1 β (IL1β) and Interleukin 1 receptor type I (IL1R), respectively, showed increased expression in SAMP8-null compared to SAMR1-null mice. SAMP8 injected with the vector coding for proinsulin displayed similar expression levels than SAMR1-null mice. (B) Protein levels of the astrocyte reactivity marker GFAP were reduced in mice treated with AAV-hPi. SAMP8-hPi showed levels of GFAP similar to those of SAMR1 mice. (C) GFAP immunofluorescence images of the hippocampus of SAMP8-null and SAMP8-hPi; CA3 area; representative images from 3 mice per group; scale bar = 200 μm. (D) Protein levels of the microglia reactivity marker Iba1 showed a non-significant trend to increase after AAV-hPi injection. (E) Iba1 immunofluorescence images of the hippocampus of SAMP8-null and SAMP8-hPi; CA3 area; representative images from 3 mice per group; scale bar = 200 μm. In A, B and D, values represent the mean ± SEM. Statistics: two-way ANOVA (repeated measures in A and univariate in B and D); $^{\&\&}P < 0.01$ effect of factor strain, $^{\$\$}P < 0.01$ effect of factor treatment; $^{**}P < 0.01$ compared to SAMR1-null and $^{\#\#}P < 0.01$ compared to SAMP8-hPi by simple main effect analysis of strain and treatment, respectively.

Figure 4. Proinsulin protected SAMP8 against cognitive impairment. (A) In the *Novel object recognition test*, SAMP8 mice administered with control vector AAV-null did not show any preference for a new object whereas those mice injected with the vector bearing the human proinsulin gene AAV-hPi recognized the new object. Memory for a new object was maintained after 24 h in SAMP8-hPi mouse group. (B) In the *Novel object location test*, all mice explored similarly two identical objects at time 0 h. After 2 h, SAMP8-null did not show preference for an object displaced to a new location whereas SAMP8-hPi mice were able to recognize the change of position and preferentially explored the displaced object. (C) In the *Morris water maze test*, SAMP8-null mice did not learn to find the escape platform during the acquisition learning nor preferentially swam in the platform quadrant at the probe trial. However those mice administered with AAV-hPi demonstrated memory capacities similar to SAMR1 mice in the probe trial. No differences in the average swimming speed were found. In all cases, values represent the mean ± SEM. Statistics: two-way ANOVA; $^{\&}P < 0.05$, $^{\&\&}P < 0.01$ effect of strain factor; $^{\$\$}P < 0.01$ effect of treatment factor; $^{**}P < 0.01$ compared to SAMR1 and $^{\#\#\#}P < 0.001$ compared to SAMP8-null by simple main effect analysis.

Figure 5. Network of the connectivity between learning and memory, neuroplasticity markers, neuroprotective and neurotrophic signaling, neuroinflammation, reactive gliosis, amyloid and tau pathology, and levels of human proinsulin. Levels of human proinsulin were the result of human proinsulin secreted from gastrocnemius muscles transduced with AAV-hPi. Nodes show the variables measured in the study and links indicate positive (continuous line) or negative (dotted line) correlations between pairs of them (Pearson's, at least $P < 0.05$). Links with greater thickness indicate higher correlation value. Nodes with greater size indicate higher centrality of the variables in the network. Centrality rank of the variables obtained by graph algorithm resulted as follows: 1, GFAP protein levels; 2, time in platform quadrant in the probe test of memory, MWM; 3, p-CREB/CREB protein ratio; 4, discrimination index at 24 h in NORT; 5, pro-BDNF protein; 6, human proinsulin in blood serum; 7, AβPP protein; 8, CREB protein; 9, p-ATF1 protein; 10, p-ERK protein; 11, p-GSK3β; 12, distance swam to find the escape platform at day 6 in acquisition of learning, MWM; 13, ERK protein; 14, IL1R mRNA; 15, discrimination index at 2 h in NORT; 16, p-CREB protein; 17, synaptophysin protein; 18, p-NFκB p65 protein; 19, discrimination index at 2 h in OLT; 20, p-ERK/ERK protein ratio; 21, TNFα mRNA; 22, BDNF protein; 23, A2M mRNA; 24, IL-1β mRNA; 25, p-Akt Thr308 protein; 26, p-tau protein; 27, p-Akt Ser473

protein; 28, Iba1 protein. The parameters are classified as follows: discrimination index at 2 h in NORT, discrimination index at 24 h in NORT, discrimination index at 2 h in OLT, distance swam to find the escape platform at day 6 in acquisition of learning in MWM, and time in platform quadrant in the probe test of memory in Learning and memory; synaptophysin protein, pro-BDNF protein and BDNF protein in Neuroplasticity; p-ERK protein, ERK protein, p-ERK/ERK protein ratio, p-Akt Thr308 protein, p-Akt Ser473 protein, p-GSK3β, p-ATF1 protein, p-CREB protein, CREB protein and p-CREB/CREB protein ratio in Neuroprotective and neurotrophic signaling; p-NFκB p65 protein, A2M mRNA, IL-1β mRNA, TNFα mRNA and IL1R mRNA in Neuroinflammation; Iba1 protein and GFAP in Reactive gliosis; and AβPP protein and p-tau protein in Amyloid and tau pathology.

Figure-1

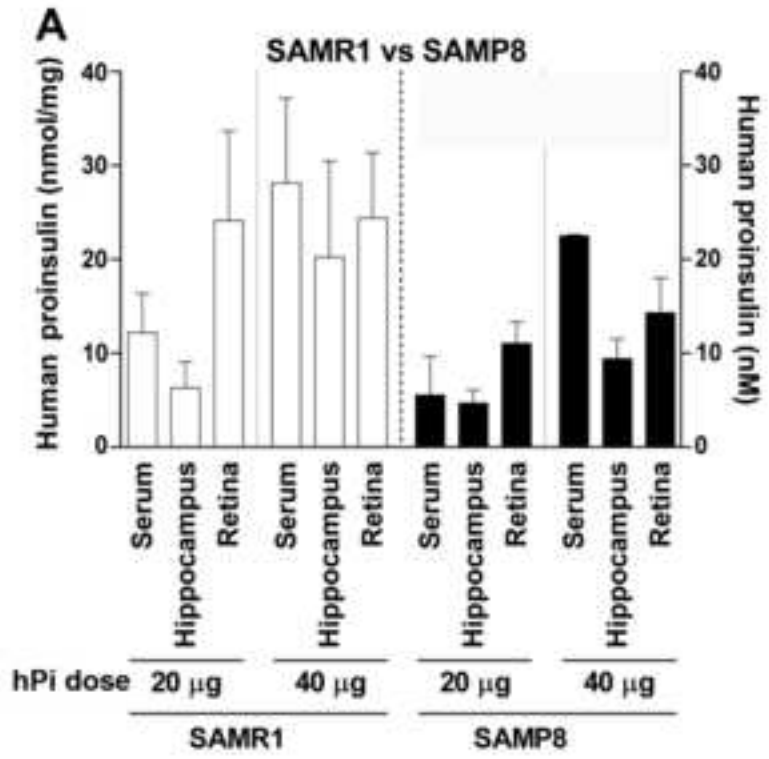
A
SAMR1 vs SAMP8
Human proinsulin (nmol/mg)
Human proinsulin (nM)
0
10
20
30
40
Serum
Hippocampus
Retina
hPi dose
20 µg
40 µg
SAMR1
SAMP8

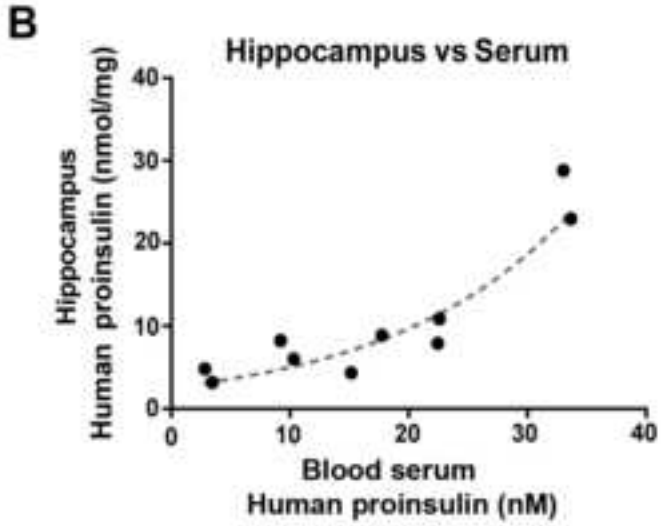
B
Hippocampus vs Serum
Hippocampus
Human proinsulin (nmol/mg)
0
10
20
30
40
Blood serum
Human proinsulin (nM)

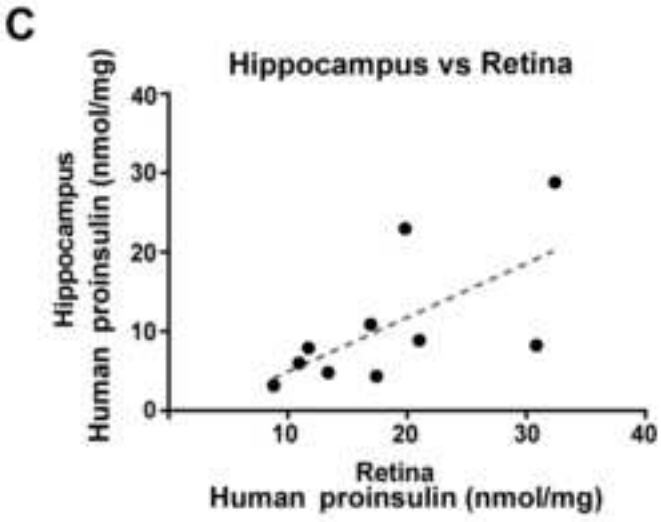
C
Hippocampus vs Retina
Hippocampus
Human proinsulin (nmol/mg)
0
10
20
30
40
Retina
Human proinsulin (nmol/mg)

Figure-2

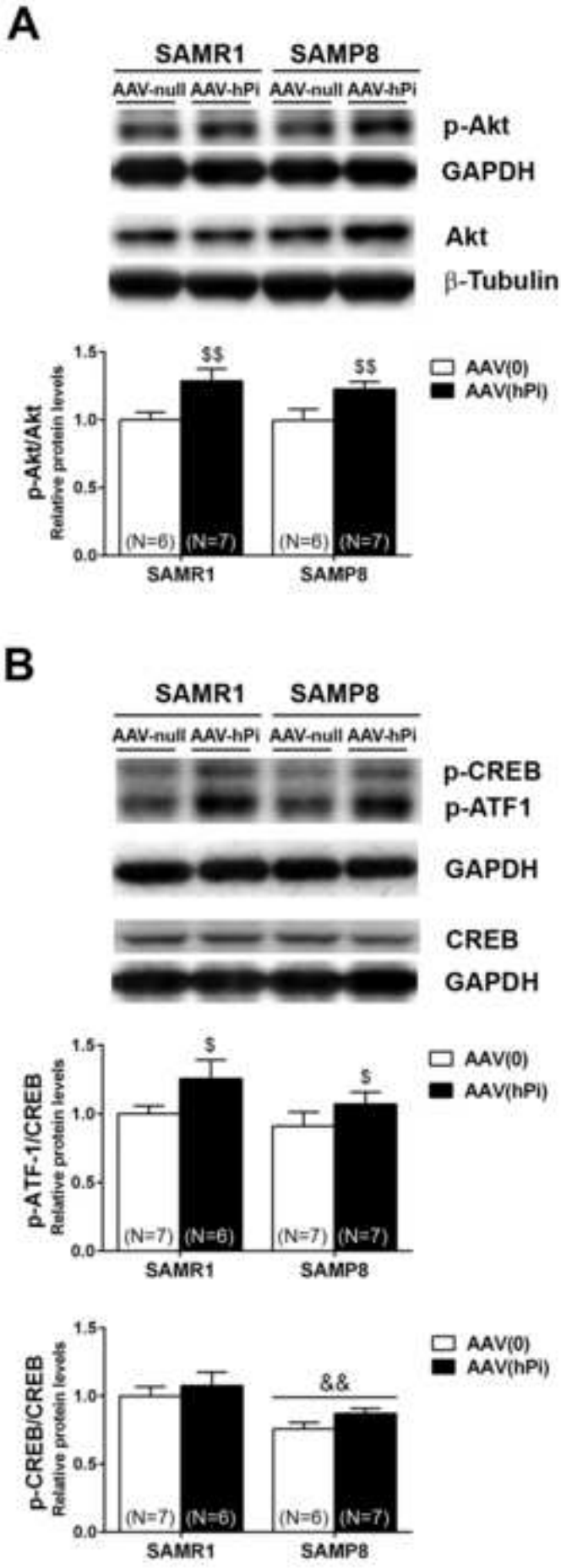
A
SAMR1
SAMP8
AAV-null
AAV-hPi
AAV-null
AAV-hPi
p-Akt
GAPDH
Akt
β-Tubulin
p-Akt/Akt
Relative protein levels
1.5
1.0
0.5
0.0
$$
$$
(N=6)
(N=7)
(N=6)
(N=7)
SAMR1
SAMP8
AAV(0)
AAV(hPi)
B
SAMR1
SAMP8
AAV-null
AAV-hPi
AAV-null
AAV-hPi
p-CREB
p-ATF1
GAPDH
CREB
GAPDH
p-ATF-1/CREB
Relative protein levels
1.5
1.0
0.5
0.0
$
$
(N=7)
(N=6)
(N=7)
(N=7)
SAMR1
SAMP8
AAV(0)
AAV(hPi)
p-CREB/CREB
Relative protein levels
1.5
1.0
0.5
0.0
&&
(N=7)
(N=6)
(N=6)
(N=7)
SAMR1
SAMP8
AAV(0)
AAV(hPi)

Figure-3

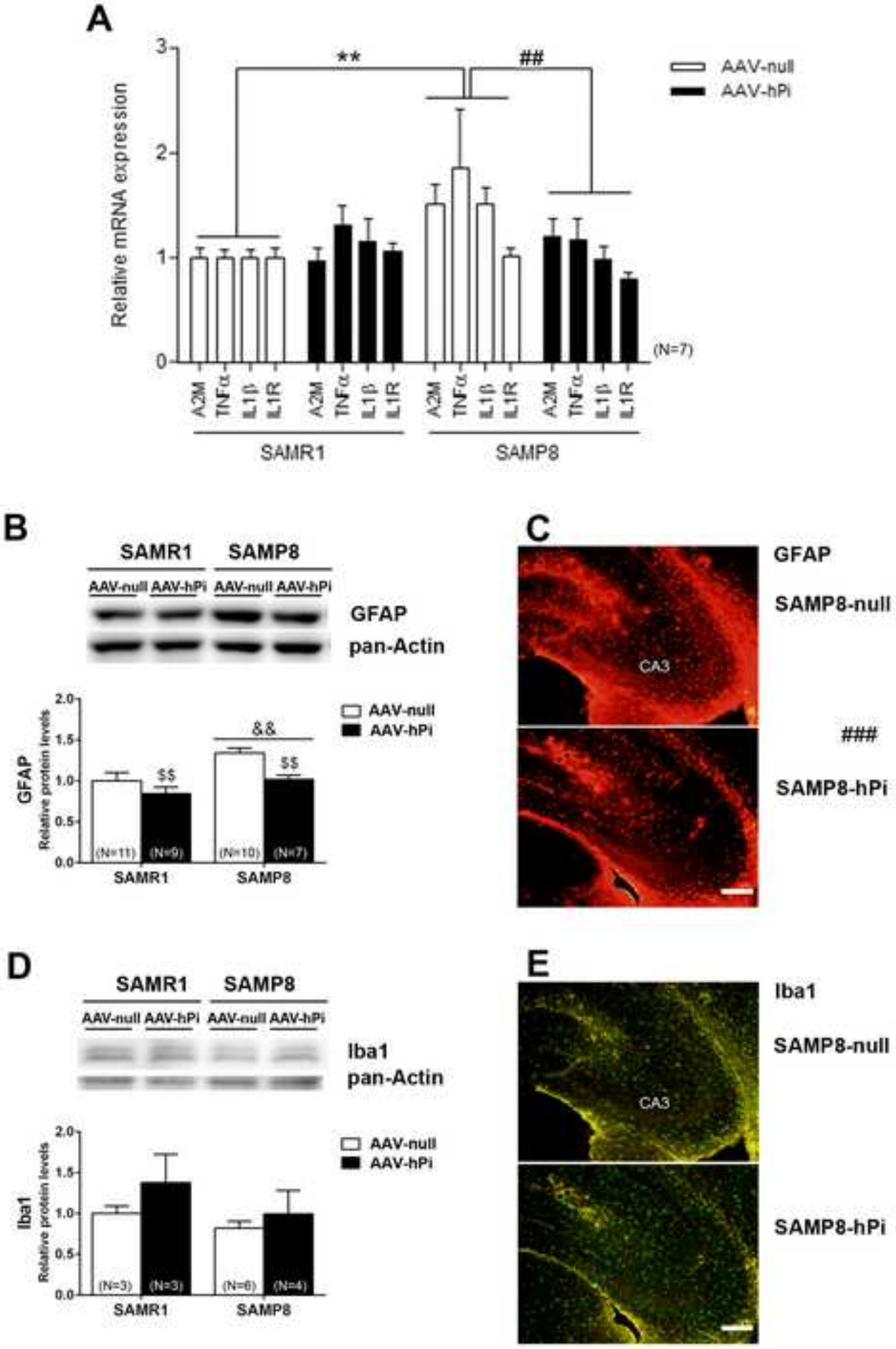
A
Relative mRNA expression
AAV-null
AAV-hPi
**
##
(N=7)
A2M
TNFα
IL1β
IL1R
SAMR1
SAMP8
B
SAMR1
SAMP8
AAV-null
AAV-hPi
GFAP
pan-Actin
GFAP
Relative protein levels
&&
$$
(N=11)
(N=9)
(N=10)
(N=7)
C
GFAP
SAMP8-null
CA3
###
SAMP8-hPi
D
Iba1
pan-Actin
(N=3)
(N=3)
(N=6)
(N=4)
E
Iba1
SAMP8-null
SAMP8-hPi

Figure-4

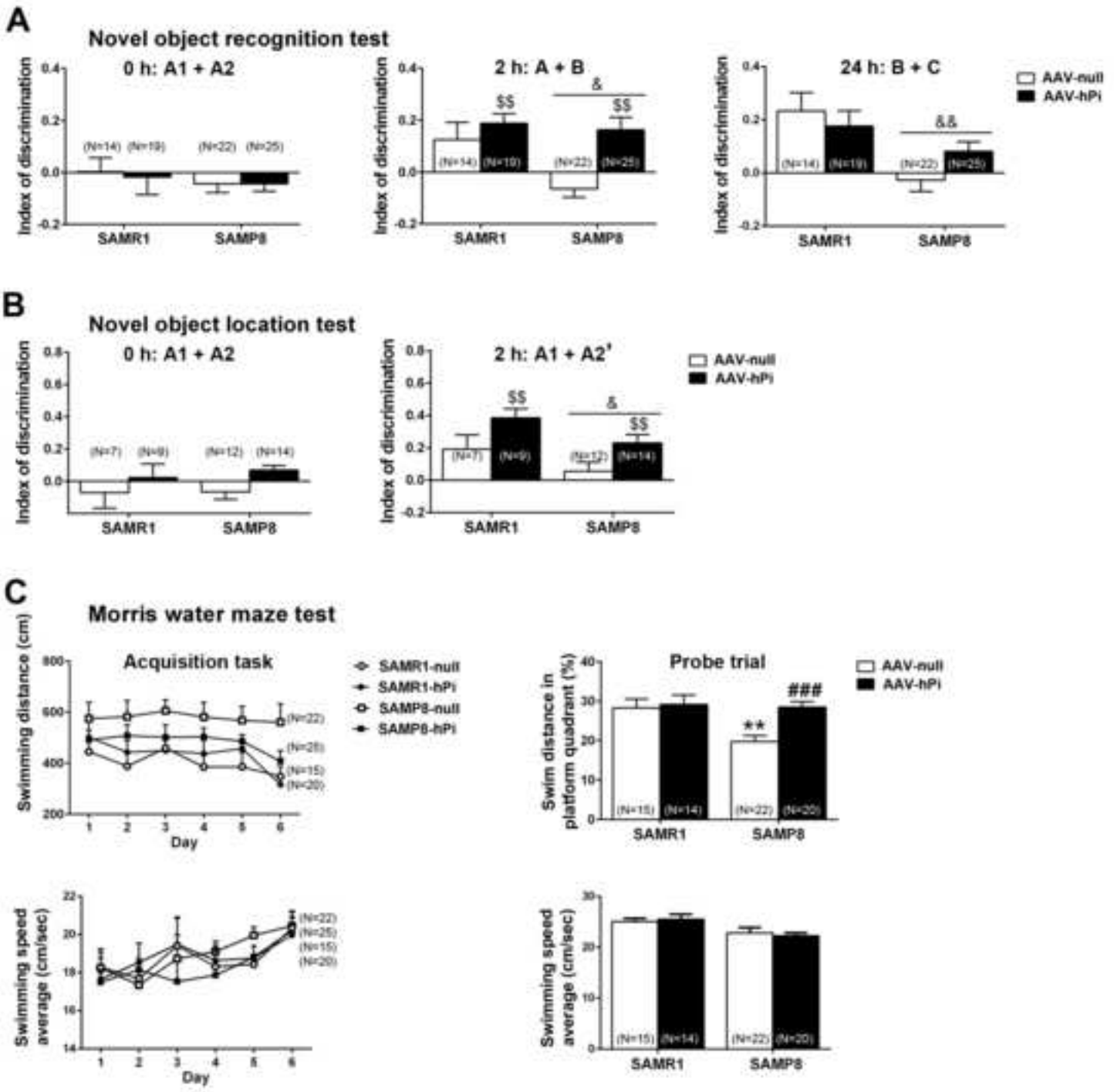
A
Novel object recognition test
0 h: A1 + A2
2 h: A + B
24 h: B + C
Index of discrimination
SAMR1
SAMP8
AAV-null
AAV-hPi
B
Novel object location test
0 h: A1 + A2
2 h: A1 + A2'
C
Morris water maze test
Acquisition task
Swimming distance (cm)
Day
SAMR1-null
SAMR1-hPi
SAMP8-null
SAMP8-hPi
Probe trial
Swim distance in platform quadrant (%)
Swimming speed average (cm/sec)

Figure-5

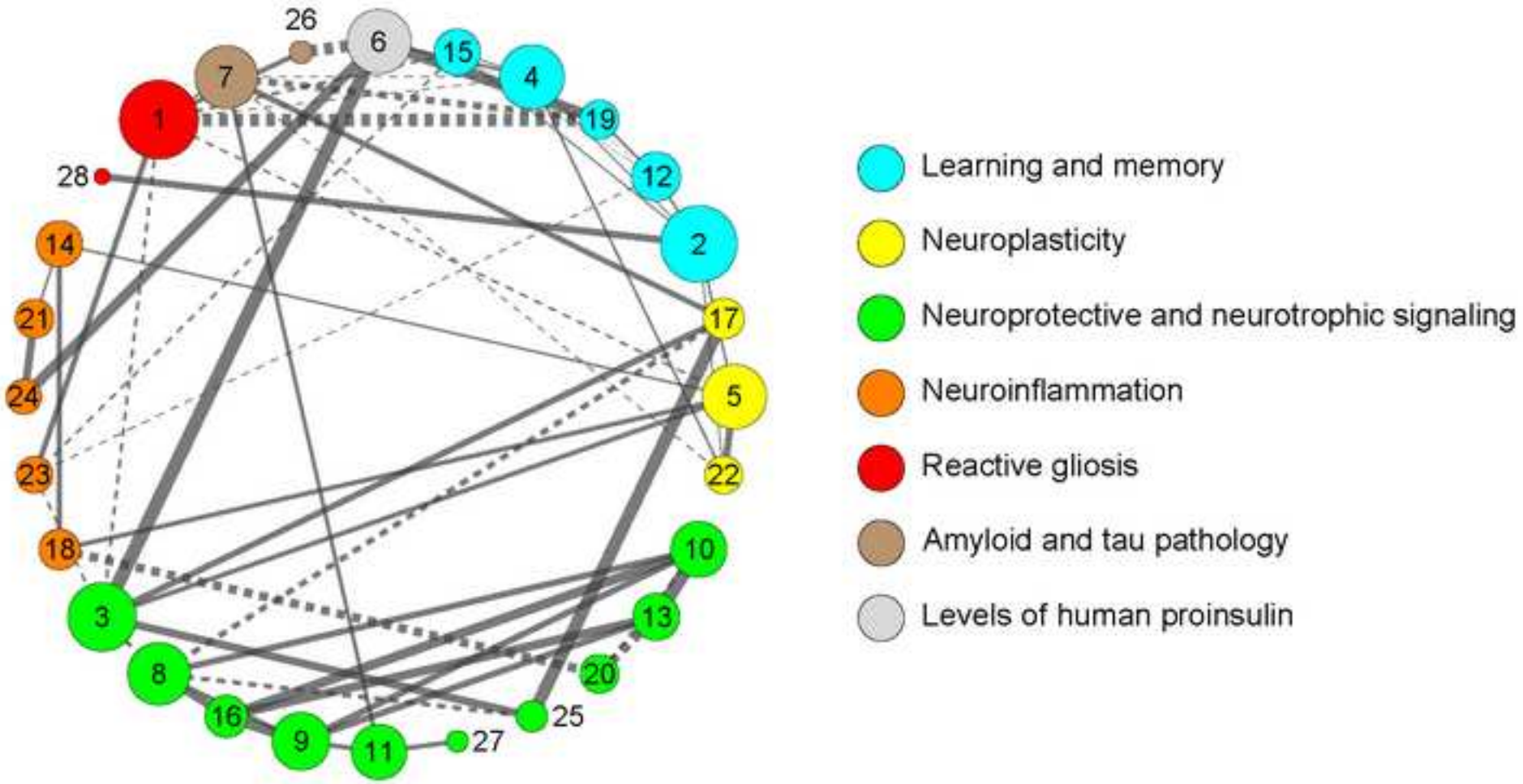
26
6
15
4
7
1
19
12
28
2
14
17
21
5
24
22
23
18
10
3
13
8
20
16
25
9
11
27
Learning and memory
Neuroplasticity
Neuroprotective and neurotrophic signaling
Neuroinflammation
Reactive gliosis
Amyloid and tau pathology
Levels of human proinsulin